to support anchorage-independent growth will provide a good experimental system for revealing the function of the negative regulatory domain of HBx, as no host factor has been reported to interact specifically with the D5 region.

Our results clearly indicate that HBx retains the ability to overcome RAS-induced senescence in human cells immortalized by hTERT, although HBx alone could neither immortalize nor transform human cells. The ability of HBx to collaborate with active RAS in cell transformation may explain its role in hepatocellular carcinogenesis. Our findings, however, were obtained using an experimental model with immortalized cells derived from human fibroblasts. Our results may not reflect the role of HBx in HBV-infected liver, as overcoming the processes of OIS seems to vary with tissue and tumor type.[41] The role of HBx should therefore be addressed using human hepatocytes and immortalized human hepatocytes. The former, however, are quite difficult to obtain whereas the latter are available at present. It had been immortalized by introducing the other viral oncogene SV LT.[42,43]

Acknowledgments

We thank K. Masutomi and W. C. Hahn for kindly providing the retroviral vectors and human immortal cell lines, T. B. S. Yen (UCSF, USA) and H. Tang (Sichuan University, China) and the members of the Division for critical discussions, and Ms Yasukawa and Ms Kuwabara for excellent technical assistance. This work was supported in part by a Grant-in-aid for Scientific Research and Development (B) (1790031) and a Grant-in-aid for Scientific Research on Priority Areas (C) (12213050 and 17013035) from the Ministry of Education, Culture, Sports, and Technology.

References

1 Seeger C, Mason WS. Hepatitis B virus biology. *Microbiol Mol Biol Rev* 2000; **64**: 51–68.
2 Nassal M, Schaller H. Hepatitis B virus replication. *Trends Microbiol* 1993; **1**: 221–8.
3 Arbuthnot P, Kew M. Hepatitis B virus and hepatocellular carcinoma. *Int J Exp Pathol* 2001; **82**: 77–100.
4 Murakami S. Hepatitis B virus X protein: structure, function and biology. *Intervirology* 1999; **42**: 81–99.
5 Murakami S. Hepatitis B virus X protein: a multifunctional viral regulator. *J Gastroenterol* 2001; **36**: 651–60.
6 Murakami S, Cheong JH, Kaneko S. Human hepatitis virus X gene encodes a regulatory domain that represses transactivation of X protein. *J Biol Chem* 1994; **269**: 15 118–23.
7 Lin Y, Tang H, Nomura T *et al.* The hepatitis B virus X protein is a co-activator of activated transcription that modulates the transcription machinery and distal binding activators. *J Biol Chem* 1998; **273**: 27 097–103.
8 Tang H, Delgermaa L, Huang F *et al.* The transcriptional transactivation function of HBx protein is important for its augmentation role in hepatitis B virus replication. *J Virol* 2005; **79**: 5548–56.
9 Shirakata Y, Kawada M, Fujiki Y *et al.* The X gene of hepatitis B virus induced growth stimulation and tumorigenic transformation of mouse NIH3T3 cells. *Jpn J Cancer Res* 1989; **80**: 617–21.
10 Kim YC, Song KS, Yoon G *et al.* Activated ras oncogene collaborates with HBx gene of hepatitis B virus to transform cells by suppressing HBx-mediated apoptosis. *Oncogene* 2001; **20**: 16–23.
11 Kim CM, Koike K, Saito I, Miyamura T, Jay G. HBx gene of hepatitis B virus induces liver cancer in transgenic mice. *Nature* 1991; **351**: 317–20.
12 Yu DY, Moon HB, Son JK *et al.* Incidence of hepatocellular carcinoma in transgenic mice expressing the hepatitis B virus X-protein. *J Hepatol* 1999; **31**: 123–32.
13 Gottlob K, Pagano S, Levrero M, Graessmann A. Hepatitis B virus X protein transcription activation domains are neither required nor sufficient for cell transformation. *Cancer Res* 1998; **58**: 3566–70.
14 Slagle BL, Lee TH, Medina D, Finegold MJ, Butel JS. Increased sensitivity to the hepatocarcinogen diethylnitrosamine in transgenic mice carrying the hepatitis B virus X gene. *Mol Carcinog* 1996; **15**: 261–9.
15 Terradillos O, Billet O, Renard CA *et al.* The hepatitis B virus X gene potentiates c-myc-induced liver oncogenesis in transgenic mice. *Oncogene* 1997; **14**: 395–404.
16 Artandi SE, DePinho RA. Mice without telomerase: what can they teach us about human cancer? *Nat Med* 2000; **6**: 852–5.
17 Balmain A, Harris CC. Carcinogenesis in mouse and human cells: parallels and paradoxes. *Carcinogenesis* 2000; **21**: 371–7.
18 Rangarajan A, Hong SJ, Gifford A, Weinberg RA. Species- and cell type-specific requirements for cellular transformation. *Cancer Cell* 2004; **6**: 171–83.
19 Hahn WC, Counter CM, Lundberg AS, Beijersbergen RL, Brooks MW, Weinberg RA. Creation of human tumour cells with defined genetic elements. *Nature* 1999; **400**: 464–8.
20 Wei W, Jobling WA, Chen W, Hahn WC, Sedivy JM. Abolition of cyclin-dependent kinase inhibitor p16Ink4a and p21Cip1/Waf1 functions permits Ras-induced anchorage-independent growth in telomerase-immortalized human fibroblasts. *Mol Cell Biol* 2003; **23**: 2859–70.
21 Akagi T, Sasai K, Hanafusa H. Refractory nature of normal human diploid fibroblasts with respect to oncogene-mediated transformation. *Proc Natl Acad Sci USA* 2003; **100**: 13 567–72.
22 Greenberg RA, Allsopp RC, Chin L, Morin GB, DePinho RA. Expression of mouse telomerase reverse transcriptase during development, differentiation and proliferation. *Oncogene* 1998; **16**: 1723–30.
23 Newbold RF. Genetic control of telomerase and replicative senescence in human and rodent cells. *Ciba Found Symp* 1997; **211**: 177–89.
24 Harvey M, Sands AT, Weiss RS. *et al. In vitro* growth characteristics of embryo fibroblasts isolated from p53-deficient mice. *Oncogene* 1993; **8**: 2457–67.
25 Kamijo T, Zindy F, Roussel MF. *et al.* Tumor suppression at the mouse INK4a locus mediated by the alternative reading frame product p19ARF. *Cell* 1997; **91**: 649–59.
26 Sedivy JM. Can ends justify the means? Telomeres and the mechanisms of replicative senescence and immortalization in mammalian cells. *Proc Natl Acad Sci USA* 1998; **95**: 9078–81.
27 Shay JW, Wright WE, Werbin H. Defining the molecular mechanisms of human cell immortalization. *Biochim Biophys Acta* 1991; **1072**: 1–7.
28 Bodnar AG, Ouellette M, Frolkis M *et al.* Extension of life-span by introduction of telomerase into normal human cells. *Science* 1998; **279**: 349–52.
29 Halvorsen TL, Leibowitz G, Levine F. Telomerase activity is sufficient to allow transformed cells to escape from crisis. *Mol Cell Biol* 1999; **19**: 1864–70.
30 Hahn WC. Role of telomeres and telomerase in the pathogenesis of human cancer. *J Clin Oncol* 2003; **21**: 2034–43.
31 Sharpless NE, DePinho RA. Cancer: crime and punishment. *Nature* 2005; **436**: 636–7.
32 Braig M, Lee S, Loddenkemper C *et al.* Oncogene-induced senescence as an initial barrier in lymphoma development. *Nature* 2005; **436**: 660–5.
33 Hahn WC, Dessain SK, Brooks MW *et al.* Enumeration of the simian virus 40 early region elements necessary for human cell transformation. *Mol Cell Biol* 2002; **22**: 2111–23.
34 Tang H, Oishi N, Kaneko S, Murakami S. Molecular functions and biological roles of hepatitis B virus X protein. *Cancer Sci* 2006; **97**: 977–83.
35 Pang R, Lee TK, Poon RT *et al.* Pin1 interacts with a specific serine-proline motif of hepatitis B virus X-protein to enhance hepatocarcinogenesis. *Gastroenterology* 2007; **132**: 1088–1103.
36 Elmore LW, Hancock AR, Chang SF *et al.* Hepatitis B virus X protein and p53 tumor suppressor interactions in the modulation of apoptosis. *Proc Natl Acad Sci USA* 1997; **94**: 14 707–12.
37 Lin Y, Nomura T, Yamashita T, Dorjsuren D, Tang H, Murakami S. The transactivation and p53-interacting functions of hepatitis B virus X protein are mutually interfering but distinct. *Cancer Res* 1997; **57**: 5137–42.
38 Lee DK, Park SH, Yi Y *et al.* The hepatitis B virus encoded oncoprotein pX amplifies TGF-beta family signaling through direct interaction with Smad4: potential mechanism of hepatitis B virus-induced liver fibrosis. *Genes Dev* 2001; **15**: 455–66.
39 Lee TH, Elledge SJ, Butel JS. Hepatitis B virus X protein interacts with a probable cellular DNA repair protein. *J Virol* 1995; **69**: 1107–14.
40 Leupin O, Bontron S, Schaeffer C, Strubin M. Hepatitis B virus X protein stimulates viral genome replication via a DDB1-dependent pathway distinct from that leading to cell death. *J Virol* 2005; **79**: 4238–45.
41 DePinho RA. The age of cancer. *Nature* 2000; **408**: 248–54.
42 Kobayashi N, Noguchi H, Watanabe T *et al.* A new approach to develop a biohybrid artificial liver using a tightly regulated human hepatocyte cell line. *Hum Cell* 2000; **13**: 229–35.
43 Kobayashi N, Miyazaki M, Fukaya K *et al.* Treatment of surgically induced acute liver failure with transplantation of highly differentiated immortalized human hepatocytes. *Cell Transplant* 2000; **9**: 733–5.

doi: 10.1111/j.1349-7006.2007.00579.x

Available online at www.sciencedirect.com
ScienceDirect
Biochemical and Biophysical Research Communications 361 (2007) 379–384
BBRC
www.elsevier.com/locate/ybbrc

Gene expression profiles in peripheral blood mononuclear cells reflect the pathophysiology of type 2 diabetes

Toshinari Takamura [a,*], Masao Honda [a], Yoshio Sakai [a], Hitoshi Ando [a], Akiko Shimizu [a], Tsuguhito Ota [a], Masaru Sakurai [a], Hirofumi Misu [a], Seiichiro Kurita [a], Naoto Matsuzawa-Nagata [a], Masahiro Uchikata [a], Seiji Nakamura [a,b], Ryo Matoba [b], Motohiko Tanino [b], Ken-ichi Matsubara [b], Shuichi Kaneko [a]

[a] *Department of Disease Control and Homeostasis, Kanazawa University Graduate School of Medical Science, 13-1 Takara-machi, Kanazawa, Ishikawa 920 8641, Japan*
[b] *DNA Chip Research Inc., Yokohama, Japan*

Received 19 June 2007
Available online 16 July 2007

Abstract

We hypothesized that systemically circulating peripheral blood mononuclear cells (PBMCs) reflect the pathophysiology of type 2 diabetes. PBMCs were obtained from 18 patients with type 2 diabetes and 16 non-diabetic subjects. The expression of genes in the PBMCs was analyzed by using a DNA chip followed by statistical analysis for specific gene sets for biological categories. The only gene set coordinately up-regulated by the existence of diabetes and down-regulated by glycemic control consisted of 48 genes involved in the c-Jun N-terminal kinase (JNK) pathway. In contrast, the only gene set coordinately down-regulated by the existence of diabetes, but not altered by glycemic control consisted of 92 genes involved in the mitochondrial oxidative phosphorylation (OXPHOS) pathway. Our findings suggest that genes involved in the JNK and OXPHOS pathways of PBMCs may be surrogate transcriptional markers for hyperglycemia-induced oxidative stress and morbidity of type 2 diabetes, respectively.

Keywords: c-Jun N-terminal kinase; Diabetes; DNA chip; Gene expression; Glycemic control; Oxidative stress; Mitochondria; Oxidative phosphorylation; Peripheral blood mononuclear cell

Diabetes is caused by absolute and/or relative deficiency of insulin action due to genetic disposition and environmental factors. Therefore, the diagnosis of diabetes requires a comprehensive understanding of hereditary aspects as well as habit and environmental effects. A long-term duration of diabetes causes chronic vascular complications. The underlying mechanism causing diabetic pathophysiology involves hyperglycemia itself and protein glycation. Additionally, bioactive mediators such as plasminogen activator-1, vascular endothelial growth factor, fatty acids, and adipocytokines secreted from the liver and adipose tissue can cause oxidative stress and thereby promote insulin resistance [1] and vascular complications [2]. We revealed one of the systemic manifestations of diabetes in our previous work, which showed that the hepatic gene expression profile of patients with type 2 diabetes is altered from that of patients without diabetes [3,4]. The livers of patients with type 2 diabetes had gene expression profiles indicative of increased angiogenesis, a reduced stress-defence system [3], and altered mitochondrial oxidative phosphorylation (OXPHOS) [4].

Owing to the multiple and complicated causes of the onset of diabetes, the search for conventional biomarkers that reflect diabetic pathophysiology and predict prognosis is an important issue. Glycated proteins such as haemoglobin A_{1C} HbA_{1C} and glucoalbumin are used as surrogate markers for long-term glycemic control [5,6]. Albuminuria

* Corresponding author. Fax: +81 76 234 4250.
E-mail address: ttakamura@m-kanazawa.jp (T. Takamura).

0006-291X/$ - see front matter © 2007 Elsevier Inc. All rights reserved.
doi:10.1016/j.bbrc.2007.07.006

is predictive of not only future diabetic nephropathy but also cardiovascular events [7,8]. High-sensitivity C-reactive protein (hs-CRP) has been found to be an independent indicator of coronary heart disease [9]. However, the use and clinical significance of these markers are limited.

Systemically circulating peripheral blood mononuclear cells (PBMCs) are considered to be a unique tissue affected by the host condition and may reflect oxidative stress caused by high levels of glucose, insulin, free fatty acids, and tissue-derived circulating bioactive mediators. To verify the hypothesis that the gene expression of PBMCs changes in response to diabetic circumstances, we comprehensively compared global gene expression profiles of PBMCs between patients with and without type 2 diabetes and between patients with type 2 diabetes before and after glycemic control, by using DNA microarray technology. We extracted the metabolic pathways coordinately altered in the PBMCs of patients with type 2 diabetes and identified the c-Jun N-terminal kinase (JNK) and OXPHOS pathways as surrogate transcriptional markers for hyperglycemia-induced oxidative stress and morbidity of type 2 diabetes, respectively. This finding may lead to the novel and powerful application of gene expression profile analysis of PBMCs for exploring the pathophysiology of diabetes.

Materials and methods

Patients. Eighteen patients with type 2 diabetes admitted to Kanazawa University Hospital between 2002 and 2004 and sixteen non-diabetic subjects were enrolled in this study. The clinical characteristics of the study subjects are shown in Table 1. No subjects had chronic inflammatory diseases such as collagen diseases and infectious diseases, all tested negative for the hepatitis B and C viruses, and all reported drinking less than 20 g/day of ethanol. The patients were diagnosed based on criteria established by an expert committee on the diagnosis and classification of diabetes mellitus [10]. The patients with diabetes were treated with diet therapy alone, oral hypoglycemic agents, or insulin as described in Table 1. Some patients were prescribed with agents for hypertension and dyslipidemia such as statins, angiotensin-converting enzyme inhibitors, or angiotensin II receptor type 1 blockers (Table 1). Overweight subjects were defined as those with a body mass index (BMI) $\geqslant 25\ kg/m^2$, which is the Japanese criteria of obesity [11].

All patients were treated for hyperglycemia at our outpatient clinic for 328 ± 235 days, and their blood samples were analyzed before and after glycemic control (Table 1).

All patients provided written informed consent for this study. The experimental protocol was approved by the relevant ethics committee of our institution and was carried out in accordance with the Declaration of Helsinki.

Laboratory studies. After an overnight fast, venous blood samples were withdrawn from each patient. Serum samples were assayed for plasma glucose, HbA_{1C}, total cholesterol, triglycerides, HDL cholesterol, insulin, alanine aminotransferase, aspartate aminotransferase (AST), hs-CRP, free fatty acids, and adipocytokines such as adiponectin, leptin, and tumor necrosis factor-α (TNF-α).

Isolation of RNA from PBMCs and amplification of antisense RNA. Heparinized blood samples were withdrawn from the peripheral vessels of subjects, and mononuclear cells were isolated by the Ficoll density-gradient method as previously described [12]. Total RNA was isolated from PBMC samples by using a Micro RNA isolation kit (Stratagene, La Jolla, CA) and RNeasy mini column (QIAGEN, Chatsworth, CA). Antisense RNA was synthesized and amplified using 2 μg of the isolated RNA with an Amino Allyl MessageAmp aRNA kit (Ambion, Austin, TX).

Preparation of fluorescently labelled cDNA and microarray hybridization. To label the probes, approximately 5 μg of amplified aRNA was chemically coupled to Cy3 or CY5 mono-reactive dye (Amersham) in accordance with the manufacturer's protocol. As a reference for each hybridization, we used aRNA samples prepared from the PBMCs of a 29-year-old healthy man. Reference aRNAs were labelled with Cy3, and test sample aRNAs were labelled with Cy5. Hybridization experiments were as described (http://www.dna-chip.co.jp/thesis/AceGeneProtocol.pdf). Briefly, the labelled probes were purified on Microcon 30 columns (Millipore, Bedford, MA); each mixture was concentrated to 31 μL. After fragmentation, 25 μL of 5× standard saline citrate (SSC), 5 μL of 10% sodium dodecyl sulphate, 8 μL of 50× Denhardt's solution, 1 μL of salmon sperm DNA (10 μg/μL), 20 μL of 5 M tetramethyl ammonium chloride, and 10 μL of formamide were added. Each 100-μL aliquot was used as a hybridization probe for the oligo-DNA chip (AceGene®Human Oligo Chip 30 K, HitachiSoft, Japan). The slides were covered with glass coverslips, fixed in a hybridization cassette (TeleChem, Sunnyvale, CA), and hybridized at 65 °C for 16 h. The slides were washed in 2× SSC and 0.03% sodium dodecyl sulphate for 5 min, 1× SSC for 5 min, and 0.2× SSC for 5 min.

Image analysis. The fluorescence intensity of each spot on the hybridized oligo-DNA microarray plate was obtained with a DNA microarray scan array G (Perkin-Elmer, Wellesley, MA). The images were quantified by DNASIS array v. 2.6 software (Hitachi Software Engineering Co., Ltd., Yokohama, Japan). The signal intensity of each spot was calibrated by subtracting adjacent background signals. To normalize the data, we averaged the intensities of all spots obtained with Cy3 and Cy5 in each of the 16 rectangles and adjusted the intensity of each corrected DNA spot by the average intensity ratio $Cy5/Cy3 = 1.0$. This global normalization of intensity provided a smaller variance of the Cy5/Cy3 ratio and almost equivalent results as normalization using housekeeping genes.

Hierarchical clustering of the gene expression in the patients was assessed by calculating Pearson's product-moment correlation coefficient using BRB-Array Tools software (NCBI, NIH, USA) [13]. The data were log transformed, normalized, mean centered, and applied to the average linkage clustering. The resulting dendrogram indicated the order in which patients were grouped based on the similarities of their gene expression patterns. The gene cluster data are presented graphically, and the analyzed genes are arranged as ordered by the clustering algorithm, so that genes with the most similar expression patterns are placed adjacent to each other.

Statistical analysis. All data are expressed as means ± SEM. To test the significance of expression ratios of individual genes or pathways, we used supervised analyses with a permutation-based method by using the BRB-Array Tools software [13]. This is the Class Comparison Tool based on univariate *F*-tests to find genes differentially expressed between predefined clinical groups. The permutation distribution of the *F*-statistic, based on 2000 random permutations, was also used to confirm statistical significance. We screened a total of 535 human gene sets, which included 285 BioCarta pathways, 101 KEGG pathways, and 149 gene sets previously described [14].

We normalized the expression levels of the 48 genes involved in the JNK pathway and 92 genes involved in the OXPHOS pathway to a mean of 0 and a variance of 1 across all samples. The mean centroid is the mean of the normalized gene expression levels [4,14]. A P value of <0.005 was considered significant.

Results

Patients characteristics

Clinical characteristics of the study subjects and the patients with diabetes before and after glycemic control

Table 1
Clinical characteristics of the patients with type 2 diabetes (T2DM) before (pre) and after (post) glycemic control

	Non-DM	T2DM	
		Pre	Post
No. (M:F)	16 (14:2)	18 (10:8)	18 (10:8)
Age (years)	26 ± 2	55 ± 17*	(after 328 ± 235 days)
BMI (kg/m^2)	21.1 ± 1.9	26.0 ± 5.4*	27 ± 5.1
Fasting plasma glucose (mmol/l)	4.6 ± 0.7	16.2 ± 15.4*	7.28 ± 2.11**
HbA_{1C} (%)	ND	11.0 ± 2.7	6.8 ± 1.5**
Total cholesterol (mmol/l)	4.62 ± 0.72	5.07 ± 0.85	5.04 ± 1.13
Triglyceride (mmol/l)	1.17 ± 0.60	1.80 ± 2.09	1.17 ± 0.65
HDL-cholesterol (mmol/l)	1.55 ± 0.31	1.34 ± 0.31	1.37 ± 0.31
Alanine aminotransferase (IU/l)	14 ± 8	35 ± 23 *	28 ± 15
hs-CRP (μg/dl)	0.070 ± 0.093	0.097 ± 0.088	0.13 ± 0.15
Tumor necrosis factor-α (pg/ml)	1.1 ± 0.65	1.3 ± 0.31	1.6 ± 0.53
Adiponectin (μg/ml)	8.5 ± 2.2	8.0 ± 4.7	11 ± 9
Leptin (ng/ml)	0.65 ± 0.31	12.6 ± 13.1 *	8.5 ± 2.2
Free fatty acids (mEq/L)	0.65 ± 0.31	1.0 ± 0.38*	0.94 ± 0.38
Treatments for diabetes			
Diet therapy alone		7	2
Metformin		2	1
Pioglitazone		2	2
Sulphonylureas		6	3
Insulin		5	11
Treatments for hypertension and hyperlipidaemia			
ACE-I or ARB		2	3
Statins		6	5

ACE-I, Angiotensin converting enzyme inhibitor; ARB, Angiotensin receptor type I blocker; Non-DM, Non-diabetic subjects; T2DM, Patients with type 2 diabetes. Data are expressed as means ± SD.
* $P < 0.05$ vs. Non-DM.
** $P < 0.05$ vs. Pre.

are shown in Table 1. Age, BMI, and levels of fasting plasma glucose, HbA_{1c}, alanine aminotransferase, leptin and free fatty acids were significantly increased in patients with type 2 diabetes. There were no significant differences in levels of adiponectin and inflammatory markers such as hs-CRP and TNF-α between diabetic and non-diabetic subjects (Table 1). The patients with diabetes were treated mainly with insulin and improved in glycemic control as described in Table 1. The use of drugs that may affect the gene expression in the PBMCs such as metformin, pioglitazone, angiotensin converting enzyme inhibitor, angiotensin receptor type I blocker or statins were not changed in most patients between before and after glycemic control. There were no significant differences in levels of inflammatory markers and adipocytokines between before and after glycemic control (Table 1).

Differential gene expression in PBMCs obtained from patients with type 2 diabetes mellitus

To explore whether the gene expression in PBMCs obtained from patients with type 2 diabetes differs from that of non-diabetic subjects, we applied supervised and non-supervised learning methods to classify the gene expression profiling. With a hierarchical clustering analysis, a non-supervised learning method, using 29,597 non-filtered genes, the patients were roughly clustered into three groups: patients with diabetes before glycemic control, patients with diabetes after glycemic control, and non-diabetic subjects.

Supervised learning methods based on the compound covariate predictor revealed that, among the various clinical parameters, only two clinical parameters, glycemic control and the presence of diabetes, significantly classified these patients (Supplementary Table 1). In contrast, age, gender, and BMI were not clinical determinants of gene expression profiling (data not shown).

Pathways that determine diabetes and the glycemic level

To examine which signalling pathways were evoked in PBMCs in type 2 diabetes, we compared the gene expression profiles obtained from type 2 diabetes patients and non-diabetic subjects. Moreover, we compared the gene expression in PBMCs obtained from pre-treated and post-treated patients with type 2 diabetes to explore which signalling pathway could be rescued by the treatment of type 2 diabetes. We screened a total of 535 human pathways determined by BioCarta, the KEGG pathway, and Affymetrix (http://www.affymetrix.com) and extracted the metabolic pathways that were significantly altered in the PBMCs of the subject groups (Table 2, Supplementary Table 2). Various pathways such as the OXPHOS (VOXPHOS_h), MAPK (ST_JNK_MAPK_Pathway_h), and electron transport chain pathways were significantly altered between subjects with and without diabetes (Table

2, Supplementary Table 2). On the other hand, pathways involved in the stress response, such as the MAPK, TNF signalling, apoptosis, and mTOR signalling pathways, were significantly altered after glycemic control (Table 2, Supplementary Table 2). These pathways were not significantly altered by age, gender, or BMI in the PBMCs of the patients with diabetes (data not shown).

The JNK pathway reflects hyperglycemia

The only pathway genes coordinately altered commonly by the existence of diabetes (pre-treated diabetic patients vs. non-diabetic subjects) and by glycemic control (pre-treated vs. post-treated diabetic patients), but not altered between post-treated diabetic patients and non-diabetic subjects, were the 48 genes involved in the JNK pathway (Table 2, Supplementary Table 3). With respect to individual genes, 10 of 48 genes involved in the JNK pathway were significantly up-regulated ($P < 0.05$), and 14 of 48 genes were significantly down-regulated after glycemic control ($P < 0.05$).

To further address the significance of the JNK pathway in the pathophysiology of type 2 diabetes, we computed the mean centroid of the JNK genes as previously described [4,14]. The JNK mean centroid was significantly higher in patients with diabetes compared with non-diabetic subjects and was significantly decreased after glycemic control (Fig. 1A).

We next evaluated the correlation of the expression level of JNK genes in the PBMCs and clinical or biochemical parameters of individuals with type 2 diabetes (Table 3). The JNK mean centroid in the PBMCs was significantly correlated with levels of fasting plasma glucose and A1C. Thus, the up-regulation of the JNK genes in the PBMCs may be associated with hyperglycemia.

OXPHOS pathway reflects morbidity of type 2 diabetes

The only pathway genes coordinately altered by the existence of diabetes (pre-treated diabetic patients vs. non-diabetic subjects and post-treated diabetic patients vs. non-diabetic subjects), but not altered by glycemic control (pre-treated vs. post-treated diabetic patients), were the 92 genes involved in the mitochondrial OXPHOS pathway and 96 genes involved in the electron transport chain pathway, which share most of the same genes (Table 2, Supplementary Table 4). With respect to individual genes, 30 of 92 genes involved in the OXPHOS pathway were significantly down-regulated, and no genes were significantly up-regulated in diabetes ($P < 0.05$).

The OXPHOS mean centroid was significantly down-regulated in patients with diabetes compared with non-diabetic subjects, whereas it was not significantly altered after glycemic control (Fig. 1B).

As shown in Table 3, the OXPHOS mean centroid in the PBMCs did not significantly correlate with the fasting levels of plasma glucose and HbA_{1C}. Thus, the down-regulation of OXPHOS genes may be determined genetically and may reflect the morbidity of type 2 diabetes.

Discussion

In the present study, we demonstrated the possibility that gene expression profiles in PBMCs reflect the pathophysiology of type 2 diabetes. As type 2 diabetes is a multifactorial disorder [15], a comprehensive approach

Table 2
Significantly altered pathways in diabetic PBMC

	Pathway description	No. of genes	T2DM-Pre vs. Non-DM		T2DM-Post vs. T2DM-Pre	
			LS permutation *p*	KS permutation *p*	LS permutation *p*	KS permutation *p*
1	Electron_Transport_Chain_h	96	0.0000905	0.0087215	0.3297651	0.1435376
2	VOXPHOS_h	92	0.0009636	0.0269323	0.2323794	0.0899932
3	HOXA9_DOWN_h	42	0.011004	0.0045108	0.0643224	0.2061987
4	4fcer1 Pathway_h	44	0.01321	0.0186952	0.4412977	0.4359556
5	pparaPathway_h	62	0.0165551	0.1204174	0.6542218	0.7514925
6	MAP00620_Pyruvate_metabolism_h	40	0.0169308	0.0955992	0.6148643	0.6883807
7	p38mapkPathway_h	55	0.0278384	0.0945286	0.0759194	0.184746
8	CR_IMMUNE_FUNCTION_h	57	0.0298111	0.0008373	0.5589565	0.8259213
9	keratinocytePathway_h	53	0.0298347	0.0827755	0.2315696	0.316895
10	ST_Fas_Signaling_Pathway_h	81	0.0309935	0.1369283	0.1961165	0.053945
11	metPathway_h	47	0.0314289	0.2487016	0.2889148	0.1813162
12	CBF_LEUKEMIA_DOWNING_AML_h	81	0.0356794	0.3177211	0.0464059	0.0042596
13	ST_B_Cell_Antigen_Receptor_h	48	0.0370735	0.2309135	0.1514077	0.2013602
14	ST_JNK_MAPK_Pathway_h	48	0.0463635	0.0181573	0.0082456	0.0048617
15	erkPathway_h	40	0.0473747	0.0488313	0.1155434	0.0388996
16	INSULIN_2F_DOWN_h	40	0.0529183	0.0283123	0.0496545	0.0783795
17	MAP00071_Fatty_acid_metabolism_h	46	0.0548243	0.0433901	0.9451761	0.9641461
18	bcrPathway_h	42	0.066755	0.3680323	0.5129712	0.678769
19	MAP00561_Glycerolipid_metabolism_h	54	0.0672738	0.0125806	0.9263149	0.9473428
20	integrinPathway_h	45	0.0748778	0.4564322	0.0871219	0.1522387

Non-DM, Non-diabetic subjects; Post, After glycemic control; Pre, Before glycemic control; T2DM, Patients with type 2 diabetes.

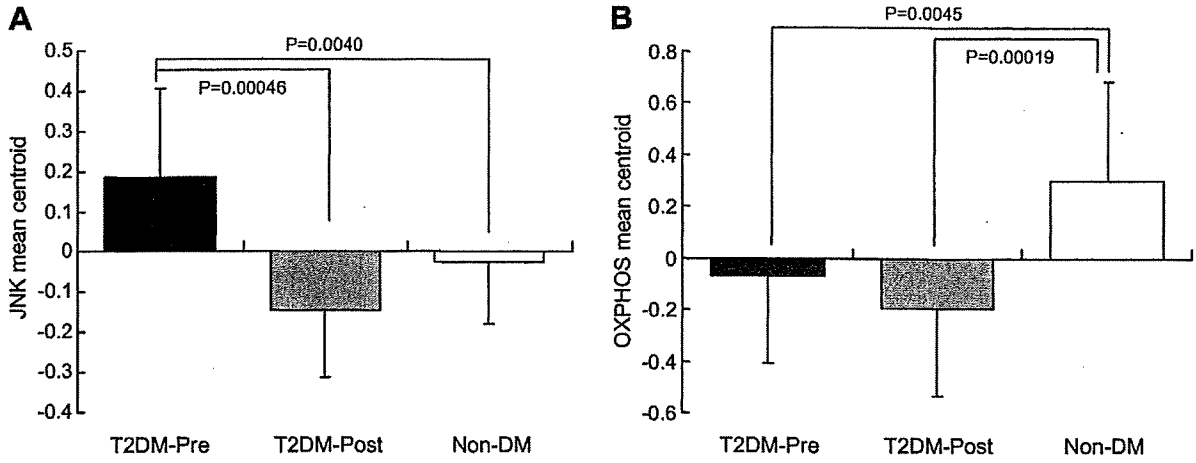

Fig. 1. JNK mean centroid (A) and OXPHOS mean centroid (B) in patients with type 2 diabetes (T2DM) before (Pre) and after (Post) glycemic control and in non-diabetic subjects (Non-DM). The mean centroid of the OXPHOS genes was computed as described in Methods. The values are means ± SD.

Table 3
Correlation of mean centroid of the genes involved in pathways for OXPHOS and JNK with the clinical parameters in patients with type 2 diabetes

	JNK mean centroid		OXPHOS mean centroid	
	Pearson's r	P	Pearson's r	P
BMI	0.018	0.920	−0.252	0.143
Fasting plasma glucose	0.468	0.018	0.097	0.644
HbA_{1C}	0.393	0.022	0.169	0.338
Fasting insulin	0.528	0.360	0.739	0.153
Alanine aminotransferase	0.232	0.208	0.127	0.496
Total cholesterol	0.154	0.417	−0.024	0.900
Triglyceride	0.098	0.606	0.093	0.624
HDL-cholesterol	0.030	0.874	0.120	0.527
hs-CRP	−0.068	0.789	−0.333	0.177
TNF-α	−0.355	0.125	−0.287	0.219
Adiponectin	−0.184	0.411	0.281	0.205
Leptin	−0.215	0.336	−0.166	0.459
Free fatty acids	0.255	0.291	0.302	0.209

identifying biological pathways or co-regulated gene sets associated with the diseases should be required to understand the molecular signature of type 2 diabetes [4]. Thus, we screened known human pathways and extracted the metabolic pathways that were significantly altered in the PBMCs of the subject groups.

We found that the distinct pathophysiology of patients with type 2 diabetes was reflected by coordinate alterations in the gene expression levels of the JNK and mitochondrial OXPHOS pathways in PBMCs; the former reflected hyperglycemia-associated oxidative stress, and the latter reflected an intrinsic alteration in patients with type 2 diabetes.

It has been recognized that, in endothelial cells, hyperglycemia causes mitochondrial superoxide production that leads to oxidative stress via glucose-induced activation of protein kinase C, increased formation of glucose-derived advanced glycation end-products, and increased glucose flux through the aldose reductase pathway [2]. Such diabetes- or hyperglycemia-induced oxidative stress may cause endoplasmic reticulum stress leading to activation of the JNK pathway in pancreatic beta-cells and hepatocytes [16]. The activation of JNK suppresses insulin biosynthesis and interferes with insulin action. Indeed, the suppression of JNK in diabetic mice was found to improve insulin resistance and ameliorate glucose tolerance [16]. Thus, the JNK pathway plays a central role in the pathogenesis of type 2 diabetes and could be a potential target for diabetes therapy. This glucose-induced oxidative stress can occur systemically, especially in PBMCs that uptake glucose in an insulin-independent manner. In the present study, the genes involved in the JNK pathway of the PBMCs were coordinately up-regulated in diabetes and significantly down-regulated after glycemic control, whereas the inflammatory markers (hs-CRP and TNF-α) and adipocytokines (adiponectin and leptin) were not altered. Thus, it might be possible that we can estimate the glucose-induced oxidative stress in pancreatic beta cells, hepatocytes, and endothelial cells simply by analyzing the gene expression profile in the PBMCs of patients with type 2 diabetes.

On the other hand, the OXPHOS pathway may predict the existence of diabetes because it was coordinately down-regulated in the PBMCs of patients with type 2 diabetes,

but was not altered by glycemic control. Emerging evidence supports the potentially unifying hypothesis that insulin secretory failure and insulin resistance, both of which are prominent features of type 2 diabetes, are caused by mitochondrial dysfunction [17]. Indeed, type 2 diabetes is associated with the coordinate down-regulation of genes involved in OXPHOS in skeletal muscle [14] and adipose tissue [18]. This alteration might occur genetically and systemically in patients with type 2 diabetes, except in the liver in which excess metabolites of glucose and fatty acids may up-regulate the genes involved in OXPHOS [4]. Thus, it might be possible to predict the predisposition or onset of type 2 diabetes simply by analyzing the gene expression profile of PBMCs.

Although future studies are necessary to clarify the effects of age, gender, type of diabetes, complications, treatment regimens for diabetes, other pharmacological treatments for hypertension and hyperlipidemia, etc., the present study suggests the diagnostic potential of gene expression analysis of PBMCs in patients with type 2 diabetes.

Appendix A. Supplementary data

Supplementary data associated with this article can be found, in the online version, at doi:10.1016/j.bbrc.2007.07.006.

References

[1] C. de Luca, J.M. Olefsky, Stressed out about obesity and insulin resistance, Nat. Med. 12 (2006) 41–42.
[2] T. Nishikawa, D. Edelstein, X.L. Du, S. Yamagishi, T. Matsumura, Y. Kaneda, M.A. Yorek, D. Beebe, P.J. Oates, H.P. Hammes, I. Giardino, M. Brownlee, Normalizing mitochondrial superoxide production blocks three pathways of hyperglycaemic damage, Nature 404 (2000) 787–790.
[3] T. Takamura, M. Sakurai, T. Ota, H. Ando, M. Honda, S. Kaneko, Genes for systemic vascular complications are differentially expressed in the livers of Type 2 diabetic patients, Diabetologia (2004).
[4] H. Misu, T. Takamura, N. Matsuzawa, A. Shimizu, T. Ota, M. Sakurai, H. Ando, K. Arai, T. Yamashita, M. Honda, T. Yamashita, S. Kaneko, Genes involved in oxidative phosphorylation are coordinately upregulated with fasting hyperglycaemia in livers of patients with type 2 diabetes, Diabetologia 50 (2007) 268–277.
[5] Y. Tahara, K. Shima, Kinetics of HbA1c, glycated albumin, and fructosamine and analysis of their weight functions against preceding plasma glucose level, Diabetes Care 18 (1995) 440–447.
[6] The relationship of glycemic exposure (HbA1c) to the risk of development and progression of retinopathy in the diabetes control and complications trial, Diabetes 44 (1995) 968–983.
[7] H.C. Gerstein, J.F. Mann, Q. Yi, B. Zinman, S.F. Dinneen, B. Hoogwerf, J.P. Halle, J. Young, A. Rashkow, C. Joyce, S. Nawaz, S. Yusuf, Albuminuria and risk of cardiovascular events, death, and heart failure in diabetic and nondiabetic individuals, Jama 286 (2001) 421–426.
[8] A.I. Adler, R.J. Stevens, S.E. Manley, R.W. Bilous, C.A. Cull, R.R. Holman, Development and progression of nephropathy in type 2 diabetes: the United Kingdom Prospective Diabetes Study (UKPDS 64), Kidney Int. 63 (2003) 225–232.
[9] J.K. Pai, T. Pischon, J. Ma, J.E. Manson, S.E. Hankinson, K. Joshipura, G.C. Curhan, N. Rifai, C.C. Cannuscio, M.J. Stampfer, E.B. Rimm, Inflammatory markers and the risk of coronary heart disease in men and women, N. Engl. J. Med. 351 (2004) 2599–2610.
[10] Expert committee on the diagnosis and classification of diabetes mellitus, Report of the expert committee on the diagnosis and classification of diabetes mellitus, Diabetes Care 26 Suppl. 1 (2003) S5-20.
[11] T. Ota, T. Takamura, N. Hirai, K. Kobayashi, Preobesity in World Health Organization classification involves the metabolic syndrome in Japanese, Diabetes Care 25 (2002) 1252–1253.
[12] M. Tateno, M. Honda, T. Kawamura, H. Honda, S. Kaneko, Expression profiling of peripheral blood mononuclear cells from patients with chronic hepatitis C undergoing interferon therapy, J. Infect. Dis. 195 (2007) 255–267.
[13] Q.H. Ye, L.X. Qin, M. Forgues, P. He, J.W. Kim, A.C. Peng, R. Simon, Y. Li, A.I. Robles, Y. Chen, Z.C. Ma, Z.Q. Wu, S.L. Ye, Y.K. Liu, Z.Y. Tang, X.W. Wang, Predicting hepatitis B virus-positive metastatic hepatocellular carcinomas using gene expression profiling and supervised machine learning, Nat. Med. 9 (2003) 416–423.
[14] V.K. Mootha, C.M. Lindgren, K.F. Eriksson, A. Subramanian, S. Sihag, J. Lehar, P. Puigserver, E. Carlsson, M. Ridderstrale, E. Laurila, N. Houstis, M.J. Daly, N. Patterson, J.P. Mesirov, T.R. Golub, P. Tamayo, B. Spiegelman, E.S. Lander, J.N. Hirschhorn, D. Altshuler, L.C. Groop, PGC-1alpha-responsive genes involved in oxidative phosphorylation are coordinately downregulated in human diabetes, Nat. Genet. 34 (2003) 267–273.
[15] S. O'Rahilly, I. Barroso, N.J. Wareham, Genetic factors in type 2 diabetes: the end of the beginning? Science 307 (2005) 370–373.
[16] H. Kaneto, Y. Nakatani, D. Kawamori, T. Miyatsuka, T.A. Matsuoka, M. Matsuhisa, Y. Yamasaki, Role of oxidative stress, endoplasmic reticulum stress, and c-Jun N-terminal kinase in pancreatic beta-cell dysfunction and insulin resistance, Int. J. Biochem. Cell Biol. 37 (2005) 1595–1608.
[17] B.B. Lowell, G.I. Shulman, Mitochondrial dysfunction and type 2 diabetes, Science 307 (2005) 384–387.
[18] I. Dahlman, M. Forsgren, A. Sjogren, E.A. Nordstrom, M. Kaaman, E. Naslund, A. Attersand, P. Arner, Downregulation of electron transport chain genes in visceral adipose tissue in type 2 diabetes independent of obesity and possibly involving tumor necrosis factor-{alpha}, Diabetes 55 (2006) 1792–1799.

FEBS Letters 581 (2007) 1983–1987

Infection of human hepatocyte chimeric mouse with genetically engineered hepatitis C virus and its susceptibility to interferon

Nobuhiko Hiraga[a,b], Michio Imamura[a,b], Masataka Tsuge[a,b], Chiemi Noguchi[a,b], Shoichi Takahashi[a,b], Eiji Iwao[c], Yoshifumi Fujimoto[b,d], Hiromi Abe[b,d], Toshiro Maekawa[b,d], Hidenori Ochi[b,d], Chise Tateno[b,e], Katsutoshi Yoshizato[b,f], Akihito Sakai[g], Yoshio Sakai[g], Masao Honda[g], Shuichi Kaneko[g], Takaji Wakita[h], Kazuaki Chayama[a,b,d,*]

[a] *Department of Medicine and Molecular Science, Division of Frontier Medical Science, Programs for Biomedical Research, Graduate School of Biomedical Sciences, Hiroshima University, Hiroshima, Japan*
[b] *Liver Research Project Center, Hiroshima University, Hiroshima, Japan*
[c] *Pharmaceuticals Research Unit, Mitsubishi Pharma Corporation, Yokohama, Japan*
[d] *Laboratory for Liver Diseases, SNP Research Center, Institute of Physical and Chemical Research (RIKEN), Yokohama, Japan*
[e] *Yoshizato Project, CLUSTER, Prefectural Institute of Industrial Science and Technology Higashihiroshima, Japan*
[f] *Developmental Biology Laboratory and Hiroshima University 21th Century COE, Program for Advanced Radiation Casualty Medicine, Department of Biological Science, Graduate School of Science, Hiroshima University, Higashihiroshima, Japan*
[g] *Department of Gastroenterology, Kanazawa University Graduate School of Medicine, Kanazawa, Japan*
[h] *Department of Virology II, National Institute of Infectious Diseases, Shinjuku-ku, Japan*

Received 15 February 2007; revised 31 March 2007; accepted 5 April 2007

Available online 20 April 2007

Edited by Hans-Dieter Klenk

Abstract **We developed a reverse genetics system of hepatitis C virus (HCV) genotypes 1a and 2a using infectious clones and human hepatocyte chimeric mice. We inoculated cell culture-produced genotype 2a (JFH-1) HCV intravenously. We also injected genotype 1a CV-H77C clone RNA intrahepatically. Mice inoculated with HCV by both procedures developed measurable and transmissible viremia. Interferon (IFN) alpha treatment resulted in greater reduction of genotype 2a HCV levels than genotype 1a, as seen in clinical practice. Genetically engineered HCV infection system should be useful for analysis of the mechanisms of resistance of HCV to IFN and other drugs.**

Keywords: Human hepatocyte chimeric mouse; Human serum albumin; HCV RNA; Interferon

1. Introduction

The hepatitis C virus (HCV) infects an estimated 170 million people worldwide [1]. HCV causes persistent infection in adults leading to chronic hepatitis, liver cirrhosis, and hepatocellular carcinoma [2,3]. The most effective therapy for viral clearance is a 48-week combination therapy of pegylated interferon (IFN)-alpha and ribavirin. However, the success rate of this combination therapy is only about 50% [4]. Development of new anti-HCV drug had been severely restricted by the absence of a cell culture system that supports the efficient replication of HCV, as well as the lack of a small animal model. A cell culture system has been developed recently using a unique genotype 2a HCV gnome (JFH-1), which does not require adaptive mutations for efficient replication [5–7]. Chimpanzee was the only useful animal for the study of HCV until recently, although the availability of this model is severely restricted [8]. Recently, HCV-infected mice have been developed by inoculating HCV-infected human serum into chimeric urokinase-type plasminogen activator (uPA)-severe combined immunodeficiency (SCID) mice with engrafted human hepatocytes [9]. This HCV-infected mouse model has been reported to be useful for evaluating anti-HCV drugs such as IFN-alpha and anti-NS3 protease [10]. We have generated a human hepatocyte chimeric mouse where mouse hepatocytes were extensively replaced by human hepatocytes [11], and established a genetically engineered hepatitis B virus (HBV) system [12]. Using this mouse, we show in this paper the development of reverse genetics system of genotypes 1a and 2a after intrahepatic injection of transcribed RNA and intravenous injection of cell culture-produced virus, respectively. We also show here that HCV in these mice can be transmitted to naïve mice. Interferon treatment of these mice resulted in a greater reduction of HCV titer in genotype 2a clone infected mice than in genotype 1a infected mice. As these results are consistent with our clinical experience, we consider this model suitable for the study of resistance of HCV against IFN and other drugs.

2. Materials and methods

2.1. Generation of human hepatocyte chimeric mice and quantification of human serum albumin

Generation of the uPA$^{+/+}$/SCID$^{+/+}$ mice and transplantation of human hepatocytes were performed as described recently by our group [11,12]. All mice used in this study were transplanted with frozen

*Corresponding author. Address: Department of Medicine and Molecular Science, Division of Frontier Medical Science, Programs for Biomedical Research, Graduate School of Biomedical Sciences, Hiroshima University, 1-2-3 Kasumi, Minami-ku, Hiroshima 734-8551, Japan. Fax: +81 82 255 6220.
E-mail address: chayama@mba.ocn.ne.jp (K. Chayama).

Abbreviations: HBV, hepatitis B virus; HCV, hepatitis C virus; HSA, human serum albumin; IFN, interferon; SCID, severe combined immunodeficiency; uPA, urokinase-type plasminogen activator

0014-5793/$32.00
doi:10.1016/j.febslet.2007.04.021

human hepatocytes obtained from one donor. Infection, extraction of serum samples, and sacrifice were performed under ether anesthesia. Mouse serum concentrations of human serum albumin (HSA) correlate with the repopulation index [11], and were measured as described previously [12]. The experimental protocol was approved by the Ethics Review Committee for Animal Experimentation of Graduate School of Biomedical Sciences, Hiroshima University.

2.2. HCV RNA transcription and inoculation into chimeric mice

A plasmid containing the full-length genotype 1a HCV cDNA clone, pCV-H77C, was kindly provided by Dr. Robert H. Purcell (National Institutes of Health). Ten micrograms of plasmid DNA, linearized by *Xba*I (Promega, Madison, WI) digestion, was transcribed in a 100-μl reaction volume with T7 RNA polymerase (Promega) at 37 °C for 2 h [13], and analyzed by agarose gel electrophoresis. Each transcription mixture was diluted with 400 μl of phosphate-buffered saline (PBS) and injected into the liver of chimeric mice. Transcripts of plasmid pJFH-1 containing the full-length HCV genotype 2a were transfected into Huh7 cells as described previously [6]. Seventy-two hours after transfection, 200 μl of the culture medium was injected intravenously into the chimeric mice. IFN-treatment was also performed by intramuscular injection of diluted IFN solutions. IFN-alpha was a kind gift from Hayashibara Biochemical Labs, Inc. (Okayama, Japan). Serum samples collected every 2 weeks after inoculation were frozen at −80 °C until further analysis.

2.3. Human serum samples

For control infection experiments, human serum containing a high titer of genotype 1b HCV (2.2×10^6 copies/ml) was obtained from a patient with chronic hepatitis after obtaining a written informed consent. The individual serum samples were divided into small aliquots and separately stored in liquid nitrogen until use.

2.4. RNA extraction and amplification

RNA was extracted from serum samples by Sepa Gene RV-R (Sankojunyaku, Tokyo), dissolved in 8.8 μl RNase-free H_2O, and reverse transcribed by using a random primer (Takara Bio, Inc., Shiga, Japan) and M-MLV reverse transcriptase (ReverTra Ace, TOYOBO Co., Osaka, Japan) in a 20 μl reaction mixture according to the instructions provided by the manufacturer. One microliter of cDNA solution was amplified by Light Cycler (Roche Diagnostic, Japan, Tokyo) for quantitation of HCV. The primers used for amplification were 5′-TTTATCCAAGAAAGGACCC-3′ and 5′-TTCACGCAGAAAGCGTCTAGC-3′. The amplification conditions included initial denaturation at 95 °C for 10 min, followed by 45 cycles of denaturation at 95 °C for 15 s, annealing at 55 °C for 5 s, and extension at 72 °C for 6 s. The lower detection limit of this assay is 10^3 copies/ml. Nested PCR was used with the outer primers NC1 (5′-CAACACTACTCGGCTAGCAGT-3′) and NC2 (5′-CCTGTGAGGAACTACTGTC-3′) and inner primers cc6 (5′-TTTATCCAAGAAAGGACCC-3′) and cc7 (5′-TTCACGCAGAAAGCGTCTAGCttc-3′). The amplification condition included 35 cycles of 94 °C for 30 s, 58 °C for 1 min 30 s, and 72 °C for 1 min after 5 min of initial denaturation at 94 °C followed by 7 min of final extension using Gene Taq (Wako Pure Chemicals, Tokyo) with anti-Taq high according to the instructions provided by the manufacturer (TOYOBO).

2.5. Histochemical analysis of mouse liver

Histopathological analysis and immunohistochemical staining using an antibody against HSA (Bethyl Laboratories Inc.) were performed as described previously [12].

3. Results

3.1. High serum HCV RNA titer in human hepatocyte chimeric mice after inoculation of serum samples obtained from HCV-infected patient

We inoculated 50 μl of genotype 1b serum samples into five chimeric mice intravenously to test their susceptibility to HCV infection. All mice became positive for HCV RNA by nested PCR at 2 weeks after inoculation (Fig. 1). The viremia reached a plateau level at 6–8 weeks after infection, and persisted for more than 12 weeks.

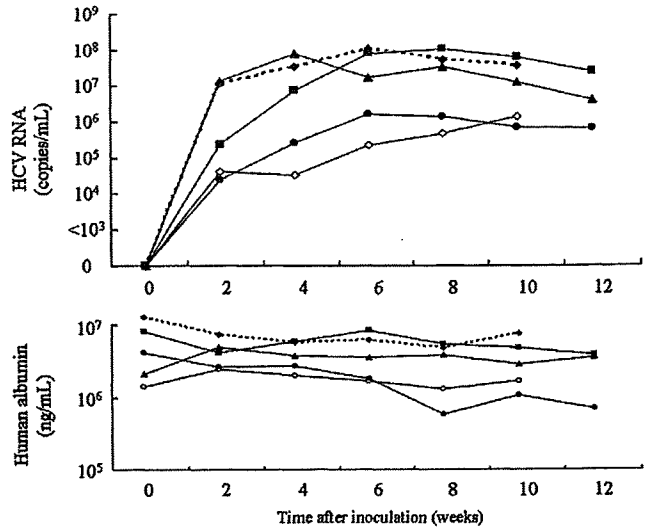

Fig. 1. Serial changes in HCV RNA and human serum albumin in sera of mice inoculated with human serum samples positive for genotype 1b HCV. Fifty microliter serum samples were injected intravenously into each mouse. Mice serum samples were obtained every 2 weeks after injection, and HCV RNA titer was analyzed.

3.2. Infection with in vitro-transcribed genotype 1a HCV RNA and cell culture generated genotype 2a HCV

In the next step, we tried to establish infection of cloned HCV using infectious genotype 1a and genotype 2a clones. In these experiments, we used two different strategies to establish infection using these two clones because genotype 1a has not been confirmed to replicate in cell culture system. We used genotype 1a HCV RNA (CV-H77C), which has been reported to be infectious to chimpanzee [13]. In vitro-transcribed HCV RNA was directly injected intrahepatically in three chimeric mice. We also infected three chimeric mice by intravenous injection of Huh7 cell-produced genotype 2a HCV after transfection of in vitro transcribed RNA from an infectious clone JFH-1. This clone has been shown to be infectious to a chimpanzee [6] and a chimeric mouse [7]. All mice developed measurable viremia 2 weeks after inoculation. At 6 weeks after inoculation, HCV RNA titer was 2.4×10^7 copies/ml (range: 8.8×10^6–2.9×10^7 copies/ml) in genotype 1a HCV-infected mice, and 2.5×10^5 copies/ml (range: 1.4×10^5–3.7×10^5 copies/ml) in genotype 2a HCV-infected mice (Fig. 2).

3.3. Passage experiment of HCV to naïve chimeric mice

We then performed passage experiments using naïve mice. Each of three mice was inoculated intravenously with 10 μl serum samples obtained from the above genotype 1a and genotype 2a HCV-infected mice at week 6. Two weeks after injection, all mice developed measurable viremia, and the titer was 8.5×10^6 copies/ml (range: 1.4×10^6–2.4×10^7 copies/ml) in genotype 1a, and 1.7×10^5 copies/ml (range: 1.5×10^5–2.5×10^5 copies/ml) in genotype 2a HCV-infected mice (Fig. 3).

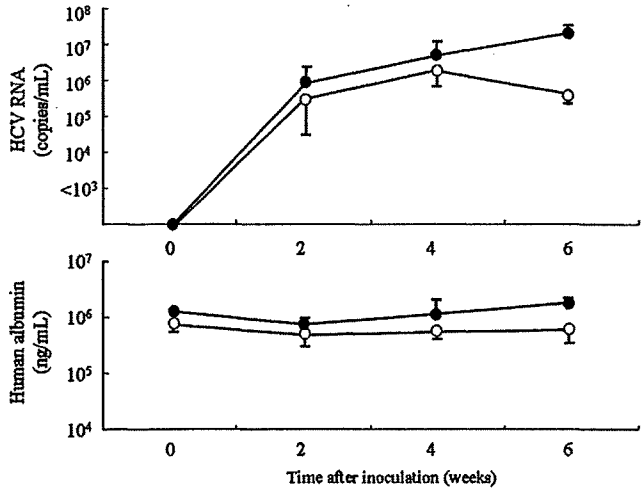

Fig. 2. Changes in HCV RNA and human albumin concentrations in serum of mice infected with clonal HCV. Each of three mice were inoculated intrahepatically with in vitro transcribed genotype 1a HCV RNA (closed circles) or intravenously with a culture medium collected from Huh7 cells transfected with JFH-1 genome intravenously (open circles). Data are mean ± S.D.

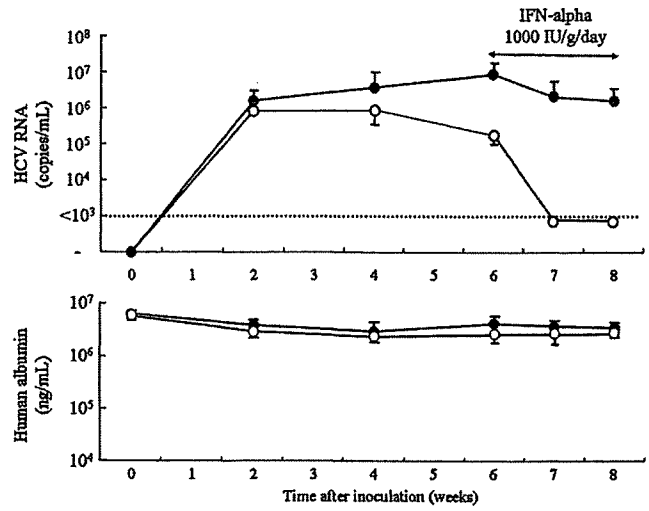

Fig. 3. Passage experiment and response to IFN-alpha therapy in mice infected with HCV genotypes 1a and 2a clones. Serum samples (10 μl) obtained from genotype 1a and 2a clonal HCV-infected mice sera (see Fig. 2) were inoculated intravenously into each of three naïve chimeric mice. Six weeks after infection, all six mice were injected intramuscularly with 1000 IU/g/day of IFN-alpha daily for 2 weeks. Closed circles: genotype 1a HCV-infected mice, open circles: genotype 2a HCV-infected mice. Data are mean ± S.D.

3.4. Variable susceptibility of HCV clones to IFN therapy

We treated each of the three mice infected with genotype 1a and 2a clones by passage experiments with 1000 IU/g of IFN-alpha daily for 2 weeks. Such treatment induced only a slight decrease in HCV in genotype 1a-infected mice; the viral load decreased only 0.6 and 0.7 log after 1 and 2 weeks of treatment, respectively (Fig. 3). In contrast, the same treatment reduced HCV genotype 2a RNA to undetectable levels after 1 and 2 weeks of IFN therapy. During IFN-treatment, serum HSA levels did not decrease in mice infected with genotype 1a or 2a HCV. Histopathological examination showed no morphological changes or apoptotic hepatocytes in replaced

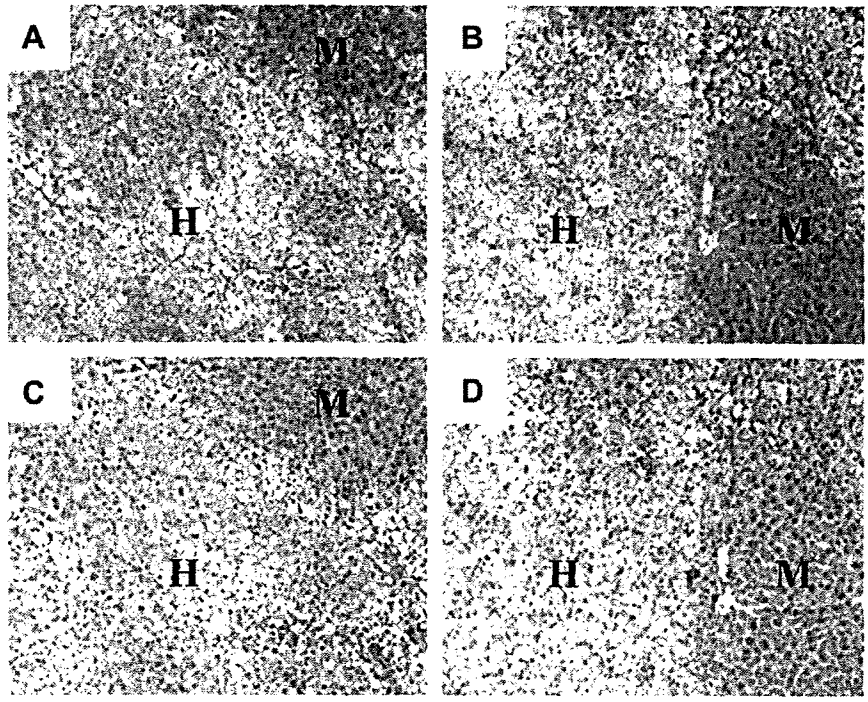

Fig. 4. Histochemical analysis of the tissues of infected chimeric mice. Liver samples obtained from mice infected with genotype 1a (A, C) and genotype 2a (B, D) stained with hematoxylin–eosin staining (A, B) or by immunohistochemical staining with anti-human serum albumin antibody (C, D). Regions are shown as human (H) and mouse (M) hepatocytes, respectively. (Original magnification, ×100.)

human hepatocytes in mice infected with each genotype after 2-week IFN-treatment (Fig. 4). These results suggest that the decrease in HCV is due to the direct anti-viral effect of IFN and not induced by liver cell damage. The difference in the virus titer and susceptibility to IFN are considered to be due to the characteristics of the genotypes.

4. Discussion

In this study, we established a reverse genetics system of HCV genotype 1a and 2a clones using human hepatocyte chimeric mice. The HCV genotype 2a clone, JFH-1, has remarkable features, i.e., infects cultured Huh7 cell line as well as establish infection in chimeric mouse [7]. It has been reported that HCV genotype 1a clone, H77-S, also infects Huh7 cell line and produces infectious virion [14]. In the present study, we intrahepatically inoculated genotype 1a infectious clone, CV-H77C. As reported in chimpanzee [13,15–17], we were able to establish genotype 1a infection using human hepatocyte chimeric mice. Using this technique, it is hoped that we can conduct further experiments in the future using genetically engineered HCV clones. Experiments using chimeric clone described by Lindenbach et al. [7] should also provide further information regarding the variable replication property of HCV genomes. Modifying genomes with nucleotide substitutions allowed examination of the functions of HCV peptides as we showed with HBV [12].

As reported recently by Kneteman et al. [10], the mouse model system is useful for evaluating the effect of anti-HCV drugs such as IFN, protease inhibitors and polymerase inhibitors. As we showed in this study, the response to IFN therapy varied according to HCV genotype. Further experiments are necessary to determine whether differences in response to IFN are due to the different replication ability (replication level of genotype 2a clone was slightly lower than that of genotype 1b, see Figs. 2 and 3) or differences in genotypes, as has been reported in clinical studies [18]. As we showed in this study (Fig. 4), there is no hepatocyte damage or inflammation in the liver of the infected chimeric mouse. Thus, this model is suitable for the study of mechanisms involved in HCV replication and IFN resistance.

The intrahepatic injection method used in this study simplified our experiments using genetically engineered virus. This is particularly important in studies of protease inhibitors and polymerase inhibitors because HCV will easily develop resistance against these small molecule agents.

Previous studies identified amino acid sequences that correlate with different susceptibilities of genotype 1b HCV against IFN therapy, namely, interferon sensitivity determining region [19] and the PKR-eIF2 phosphorylation homology domain [20,21]. To elucidate such issues, we are currently trying to establish genotype 1b infection system using the method described in this paper.

In summary, we showed in the present study the successful application of a genetically engineered HCV in human hepatocyte chimeric mice. Using this mouse model, we showed that genotypes 1a and 2a HCV clones exhibit different susceptibilities to IFN-alpha therapy. Our mouse model seems useful for the study of HCV virology and resistance of HCV against IFN and for the development of new anti-HCV therapy.

Acknowledgements: The authors thank Rie Akiyama, Kana Kunihiro and Kiyomi Toyota for their expert technical help, Dr. Robert H. Purcell and Dr. Jens Bukh for providing the full-length HCV cDNA clone of pCV-H77C. This study was supported in part by a Grant-in-Aid for Scientific Research from Japanese Ministry of labor, Health and Welfare.

References

[1] WHO. (1999) Global surveillance and control of hepatitis C. Report of a WHO Consultation organized in collaboration with the Viral Hepatitis Prevention Board, Antwerp, Belgium. J. Viral. Hepat. 6, 35–47.

[2] Kiyosawa, K., Sodeyama, T., Tanaka, E., Gibo, Y., Yoshizawa, K., Nakano, Y., Furuta, S., Akahane, Y., Nishioka, K. and Purcell, R.H. (1990) Interrelationship of blood transfusion, non-A, non-B hepatitis and hepatocellular carcinoma: analysis by detection of antibody to hepatitis C virus. Hepatology 12, 671–675.

[3] Niederau, C., Lange, S., Heintges, T., Erhardt, A., Buschkamp, M., Hurter, D., Nawrocki, M., Kruska, L., Hensel, F., Petry, W. and Haussinger, D. (1998) Prognosis of chronic hepatitis C: results of a large, prospective cohort study. Hepatology 28, 1687–1695.

[4] Fried, M.W., Shiffman, M.L., Reddy, K.R., Smith, C., Marinos, G., Goncales Jr., F.L., Haussinger, D., Diago, M., Carosi, G., Dhumeaux, D., Craxi, A., Lin, A., Hoffman, J. and Yu, J. (2002) Peginterferon alfa-2a plus ribavirin for chronic hepatitis C virus infection. N. Engl. J. Med. 347, 975–982.

[5] Zhong, J., Gastaminza, P., Cheng, G., Kapadia, S., Kato, T., Burton, D.R., Wieland, S.F., Uprichard, S.L., Wakita, T. and Chisari, F.V. (2005) Robust hepatitis C virus infection in vitro. Proc. Natl. Acad. Sci. USA 102, 9294–9299.

[6] Wakita, T., Pietschmann, T., Kato, T., Date, T., Miyamoto, M., Zhao, Z., Murthy, K., Habermann, A., Krausslich, H.G., Mizokami, M., Bartenschlager, R. and Liang, T.J. (2005) Production of infectious hepatitis C virus in tissue culture from a cloned viral genome. Nat. Med. 11, 791–796.

[7] Lindenbach, B.D., Meuleman, P., Ploss, A., Vanwolleghem, T., Syder, A.J., McKeating, J.A., Lanford, R.E., Feinstone, S.M., Major, M.E., Leroux-Roels, G. and Rice, C.M. (2006) Cell culture-grown hepatitis C virus is infectious in vivo and can be recultured in vitro. Proc. Natl. Acad. Sci. USA 103, 3805–3809.

[8] Shimizu, Y.K., Weiner, A.J., Rosenblatt, J., Wong, D.C., Shapiro, M., Popkin, T., Houghton, M., Alter, H.J. and Purcell, R.H. (1990) Early events in hepatitis C virus infection of chimpanzees. Proc. Natl. Acad. Sci. USA 87, 6441–6444.

[9] Mercer, D.F., Schiller, D.E., Elliott, J.F., Douglas, D.N., Hao, C., Rinfret, A., Addison, W.R., Fischer, K.P., Churchill, T.A., Lakey, J.R., Tyrrell, D.L. and Kneteman, N.M. (2001) Hepatitis C virus replication in mice with chimeric human livers. Nat. Med. 7, 927–933.

[10] Kneteman, N.M., Weiner, A.J., O'Connell, J., Collett, M., Gao, T., Aukerman, L., Kovelsky, R., Ni, Z.J., Zhu, Q., Hashash, A., Kline, J., His, B., Schiller, D., Douglas, D., Tyrrell, D.L. and Mercer, D.F. (2006) Anti-HCV therapies in chimeric scid-Alb/uPA mice parallel outcomes in human clinical application. Hepatology 43, 1346–1353.

[11] Tateno, C., Yoshizane, Y., Saito, N., Kataoka, M., Utoh, R., Yamasaki, C., Tachibana, A., Soeno, Y., Asahina, K., Hino, H., Asahara, T., Yokoi, T., Furukawa, T. and Yoshizato, K. (2004) Near completely humanized liver in mice shows human-type metabolic responses to drugs. Am. J. Pathol. 165, 901–912.

[12] Tsuge, M., Hiraga, N., Takaishi, H., Noguchi, C., Oga, H., Imamura, M., Takahashi, S., Iwao, E., Fujimoto, Y., Ochi, H., Chayama, K., Tateno, C. and Yoshizato, K. (2005) Infection of human hepatocyte chimeric mouse with genetically engineered hepatitis B virus. Hepatology 42, 1046–1054.

[13] Yanagi, M., Purcell, R.H., Emerson, S.U. and Bukh, J. (1997) Transcripts from a single full-length cDNA clone of hepatitis C virus are infectious when directly transfected into the liver of a chimpanzee. Proc. Natl. Acad. Sci. USA 94, 8738–8743.

[14] Yi, M., Villanueva, R.A., Thomas, D.L., Wakita, T. and Lemon, S.M. (2006) Production of infectious genotype 1a hepatitis C virus (Hutchinson strain) in cultured human hepatoma cells. Proc. Natl. Acad. Sci. USA 103, 2310–2315.
[15] Kolykhalov, A.A., Agapov, E.V., Blight, K.J., Mihalik, K., Feinstone, S.M. and Rice, C.M. (1997) Transmission of hepatitis C by intrahepatic inoculation with transcribed RNA. Science 277, 570–574.
[16] Yanagi, M., StClaire, M., Emerson, S.U., Purcell, R.H. and Bukh, J. (1999) In vivo analysis of the 3′ untranslated region of the hepatitis C virus after in vitro mutagenesis of an infectious cDNA clone. Proc. Natl. Acad. Sci. USA 96, 2291–2295.
[17] Beard, M.R., Abell, G., Honda, M., Carroll, A., Gartland, M., Clarke, B., Suzuki, K., Lanford, R., Sangar, D.V. and Lemon, S.M. (1999) An infectious molecular clone of a Japanese genotype 1b hepatitis C virus. Hepatology 30, 316–324.
[18] McHutchison, J.G., Gordon, S.C., Schiff, E.R., Shiffman, M.L., Lee, W.M., Rustgi, V.K., Goodman, Z.D., Ling, M.H., Cort, S. and Albrecht, J.K. (1998) Interferon alfa-2b alone or in combination with ribavirin as initial treatment for chronic hepatitis C. Hepatitis Interventional Therapy Group. N. Engl. J. Med. 339, 1485–1492.
[19] Enomoto, N., Sakuma, I., Asahina, Y., Kurosaki, M., Murakami, T., Yamamoto, C., Ogura, Y., Izumi, N., Marumo, F. and Sato, C. (1996) Mutations in the non-structural protein 5A gene and response to interferon in patients with chronic hepatitis C virus 1b infection. N. Engl. J. Med. 334, 77–81.
[20] Taylor, D.R., Shi, S.T., Romano, P.R., Barber, G.N. and Lai, M.M. (1999) Inhibition of the interferon-inducible protein kinase PKR by HCV E2 protein. Science 285, 107–110.
[21] Chayama, K., Suzuki, F., Tsubota, A., Kobayashi, M., Arase, Y., Saitoh, S., Suzuki, Y., Murashima, N., Ikeda, K., Takahashi, N., Kinoshita, M. and Kumada, H. (2000) Association of amino acid sequence in the PKR-eIF2 phosphorylation homology domain and response to interferon therapy. Hepatology 32, 1138–1144.

Expression Profiling of Peripheral-Blood Mononuclear Cells from Patients with Chronic Hepatitis C Undergoing Interferon Therapy

Makoto Tateno,[1] Masao Honda,[1] Takashi Kawamura,[2] Hiroyuki Honda,[2] and Shuichi Kaneko[1]

[1]Department of Cancer Gene Regulation, Kanazawa University Graduate School of Medical Science, Kanazawa, and [2]Department of Biotechnology, School of Engineering, Nagoya University, Nagoya, Japan

Background. Interferon (IFN) is now the standard treatment for chronic hepatitis C (CH-C); however, treatment efficacy is unpredictable before IFN therapy is started.

Methods. We investigated the gene-expression profiles of peripheral-blood mononuclear cells (PBMCs) from patients with CH-C showing different responses to IFN. Gene-expression profiles of PBMCs were analyzed in 21 patients with CH-C treated with IFN alone or in combination with ribavirin as well as in 6 healthy volunteers. Serial changes in the gene-expression profiles of PBMCs from individual patients were evaluated before treatment, 2 weeks after the start of IFN therapy, and 6 months after the completion of IFN therapy.

Results. Interestingly, the gene-expression profiles of PBMCs from patients with CH-C and healthy volunteers differed substantially; early T cell–activation antigen CD69 was significantly up-regulated in patients with CH-C, but immune-related molecules such as chemokine (C-C motif) receptor 2 and interleukin 7 receptor were significantly down-regulated. Selected combinations of expressed genes obtained before treatment and during IFN therapy by use of a fuzzy neural network combined with the SWEEP operator method predicted the outcome of IFN therapy with peak accuracies of 91.0% and 90.2%, respectively.

Conclusions. These findings suggest that the gene-expression profiles of PBMCs from patients with CH-C may be useful biomarkers for IFN therapy.

Although interferon (IFN) is currently the standard treatment for patients with chronic hepatitis C (CH-C), only 30%–40% of patients completely eliminate the virus, even after effective IFN and ribavirin combination therapy [1–3]. The mechanism of viral persistence during IFN treatment remains to be clarified. It has been reported that several clinical factors, such as viral load, genotype, degree of fibrosis, and expression of type I IFN receptors, are useful predictive factors for the outcome of IFN therapy [4–6]; however, precise prediction is not possible at present.

Type I IFN, such as IFN-α and IFN-β, plays an important role in innate immunity against viral infections by suppressing viral replication [7, 8]. However, the biological activities of IFN have not been fully elucidated. In viral infections such as measles, the number of peripheral lymphocytes generally decreases. It has also been reported that infection of dendritic cells and other immunocompetent cells is involved in exacerbated disease states and persistent infection [9]. Hence, it may be possible to assess disease state and severity by examining peripheral-blood mononuclear cells (PBMCs) from infected individuals. PBMCs include lymphocytes and monocytes, which play the most important roles in the immunological response to viral infection.

In the present study, we investigated the gene-expression profiles of PBMCs from patients with CH-C and healthy volunteers by use of cDNA microarray techniques [10–16]. By determining the gene-expression profiles of PBMCs from patients with CH-C receiving IFN therapy, we also clarified the differences in the PBMC gene-expression profiles between patients

Received 30 May 2006; accepted 23 August 2006; electronically published 13 December 2006.

Potential conflicts of interest: none reported.

Reprints or correspondence: Shuichi Kaneko, Dept. of Cancer Gene Regulation, Kanazawa University Graduate School of Medical Science, 13-1, Takara-Machi, Kanazawa 920-8641, Japan (skaneko@medf.m.kanazawa-u.ac.jp).

The Journal of Infectious Diseases 2007;195:255–67

0022-1899/2007/19502-0014$15.00

Table 1. Clinical characteristics of patients and responses to interferon (IFN) therapy.

Group, patient (sex, age in years)	ALT level, IU/L	Histology score[a]	Serotype	IFN therapy	Response	Serum HCV RNA level, kIU/mL			PBMC HCV RNA at 2 weeks
						Before	2 weeks	6 months	
Group A									
1 (M, 46)	31	F1/A1	2	Mono	CR	23	<0.5	<0.5	–
2 (F, 47)	40	F1/A1	2	Mono	CR	416	<0.5	<0.5	+
3 (M, 71)	59	F4/A2	1	Mono	CR	42.3	2.2	<0.5	–
4 (M, 55)	19	F4/A2	2	Mono	CR	1.3	<0.5	<0.5	–
5 (M, 54)	30	F2/A1	1	Mono	BR	620	ND	>850	ND
6 (F, 43)	46	F2/A1	1	Mono	BR	160	<0.5	611	+
7 (M, 58)	236	F1-2/A1	NA	Mono	BR	360	<0.5	620	–
8 (M, 60)	114	F3/A2	2	Mono	BR	770	<0.5	2200	–
9 (M, 62)	70	F2/A1	1	Mono	NR	130	130	350	+
10 (M, 42)	59	F2/A1	1	Mono	NR	800	7.2	190	–
11 (F, 62)	138	F2-3/A2	2	Mono	NR	650	183	1400	+
12 (M, 49)	48	F2/A2	2	Mono	NR	330	<0.5	69.5	–
13 (F, 56)	104	F1/A1	1	Mono	NR	751	<0.5	610	–
Group B									
14 (M, 49)	69	F3/A2	1	Combination	CR	>850	ND	<0.5	ND
15 (M, 50)	35	F1/A2	1	Combination	CR	475	<0.5	<0.5	ND
16 (M, 44)	106	F2/A2	1	Combination	NR	325	68.8	82.6	ND
17 (M, 56)	30	F2/A1	1	Combination	CR	91	<0.5	<0.5	ND
18 (F, 39)	47	F1/A1	1	Combination	CR	>850	0.7	<0.5	ND
19 (F, 64)	117	F2/A1	1	Combination	NR	484	0.8	>850	ND
20 (M, 66)	31	F2/A1	1	Combination	NR	>850	390	1300	ND
21 (F, 62)	103	F3/A2	1	Combination	NR	820	270	1200	ND

NOTE. +, positive; –, negative; ALT, alanine aminotransferase; BR, biochemical responder; CR, complete responder; F, female; M, male; NA, not applicable; ND, not detected; NR, nonresponder; PBMC, peripheral-blood mononuclear cell.

[a] Grading and staging of chronic hepatitis were histologically assessed according to the method of Desmet et al. [17], as described in the text.

with CH-C who responded to IFN therapy (complete responders [CRs]) and those who did not (nonresponders [NRs]).

SUBJECTS, MATERIALS, AND METHODS

Patients. Subjects were 21 patients with CH-C and 7 patients who showed no clinical signs of hepatitis at Kanazawa University Hospital, Japan, between 1999 and 2001. To 13 patients with CH-C (group A), 6 million IUs of IFN-α2b was administered every day for 2 weeks and then 3 times weekly for 22 weeks. To 8 patients with CH-C (group B), IFN-α2b was administered in the same fashion, and ribavirin was administered concomitantly (600 mg for ≤60 kg of body weight, 800 mg for >60 and ≤80 kg of body weight, and 1000 mg for >80 kg of body weight). The 6 age- and sex-matched healthy volunteers were seronegative for either hepatitis B surface antigen or hepatitis C virus (HCV) antibody and had liver function values within normal limits. Eight CRs (negative HCV RNA for >6 months), 4 biochemical responders (BRs; normal serum alanine aminotransferase [ALT] levels for >6 months and positive serum HCV RNA), and 9 NRs to IFN therapy were enrolled. After informed consent was obtained from patients, peripheral-blood samples were collected before the start of IFN therapy, at 2 weeks into treatment, and at 6 months after the completion of treatment. PBMCs were then isolated from whole blood and stored in liquid nitrogen until use. Grading and staging of chronic hepatitis were histologically assessed according to the method of Desmet et al. [17]. Clinical characteristics, such as sex, age, ALT levels, degree of histological activity or staging, HCV RNA load and HCV serotype, did not differ significantly among the groups (table 1).

Virological assessment. The amount of HCV RNA was assayed by the Amplicor Monitor Test (Roche Molecular Systems). HCV was classified by a serologic genotyping assay that has been shown to be specific and sensitive for determining HCV genome subtype [18].

Preparation of cDNA microarray slides. Most cDNA clones used in the present study were obtained from IMAGE Consortium libraries through their distributor, Research Genetics, as described elsewhere [19–24]. In addition to these clones, we included clones to monitor IFN signaling. The newly constructed cDNA microarray slide (Kanazawa IFN chip; version 1.0) comprised 400 representative IFN signaling–related

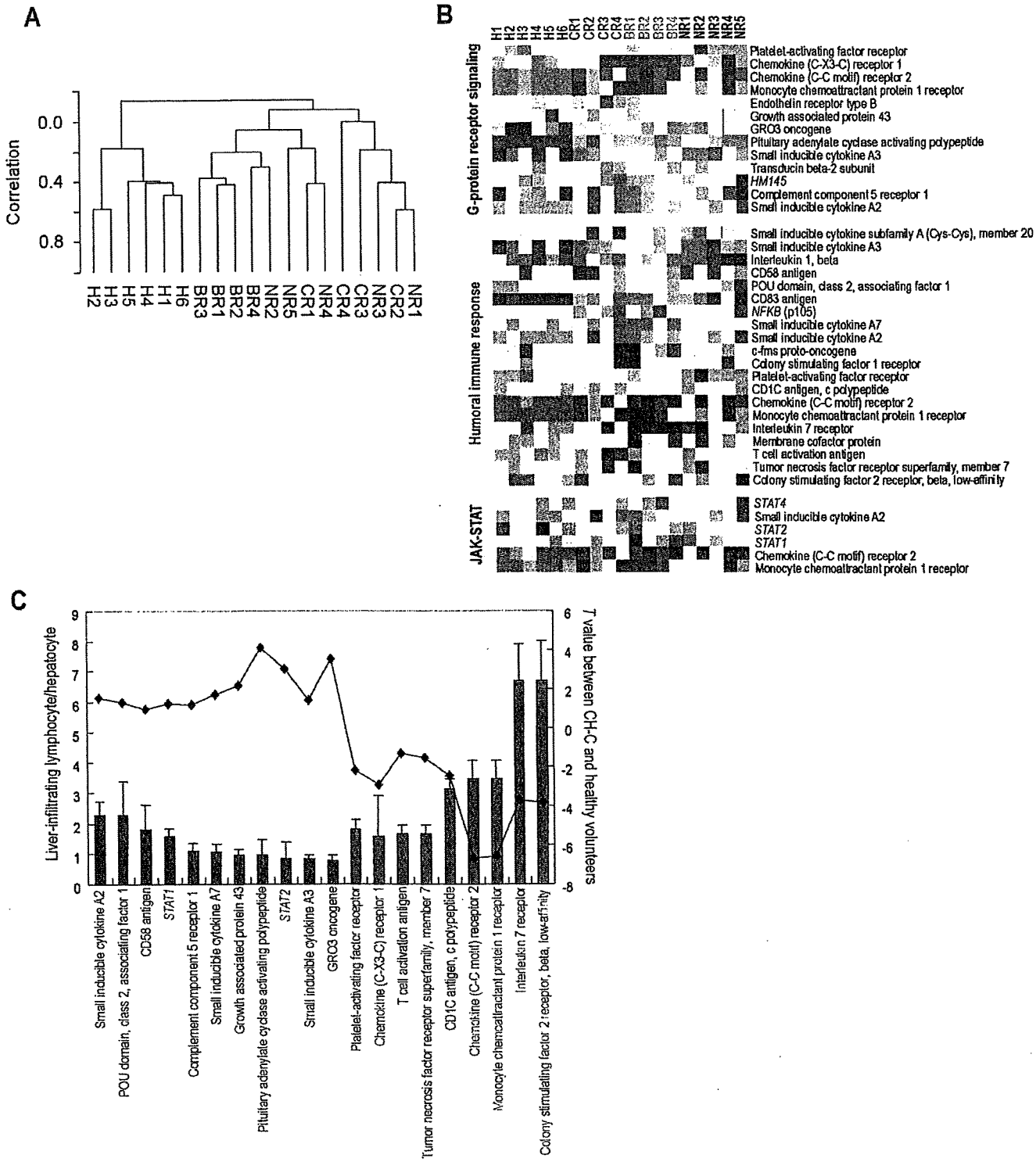

Figure 1. *A,* Hierarchical clustering analysis of gene-expression profiles of peripheral-blood mononuclear cell (PBMC) samples from 13 patients with chronic hepatitis C (CH-C; complete responders [CRs] 1–4, biochemical responders [BRs] 1–4, and nonresponders [NRs] 1–5) and 6 healthy volunteers (H1–H6) among 1305 tested genes before the start of interferon (IFN) therapy, performed using BRB-ArrayTools software. The dendrogram indicates the order in which patients were grouped on the basis of similarities in their gene-expression patterns. *B,* One-way clustering analysis of gene-expression profiles of PBMCs before the start of IFN therapy, using differentially expressed genes in the Janus kinase signal transducer and activation of transcription (JAK-STAT) cascade, humoral immune response, and G protein–coupled receptor protein signaling pathway. Gene cluster data are presented graphically as colored images; red indicates up-regulated genes, and blue indicates down-regulated genes. *C,* Bar graph indicating gene expression in liver-infiltrating lymphocytes relative to that in hepatocytes *(left axis),* and line graph indicating the *T* values for class-prediction analysis between patients with CH-C and healthy volunteers *(right axis).* Genes with increased expression in the liver *(red)* tended to be expressed at lower levels in PBMCs, and genes with decreased expression in the liver *(blue)* tended to be expressed at higher levels in PBMCs.

Table 2. Representative up- or down-regulated genes in patients with chronic hepatitis C, compared with that in healthy volunteers.

Category, gene name	Ratio	*T*	*P*	GenBank accession no.	Gene annotation
Up-regulated					
CD83 antigen (activated B lymphocytes, immunoglobulin superfamily)	3.60	4.26	.00125	NM_004233	Defense response
Thrombospondin 1	3.29	5.19	.00014	NM_003246	Endopeptidase inhibitor activity
CD69 antigen (p60, early T cell–activation antigen)	2.87	5.55	.00001	NM_001781	Transmembrane receptor activity
Regulator of G protein signaling 1	2.33	4.31	.00029	NM_002922	Signal transducer activity
Pituitary adenylate cyclase–activating polypeptide	2.01	4.12	.00046	NM_001117	Neuropeptide hormone activity
Nicotinamide N-methyltransferase	1.99	5.29	.00003	NM_006169	Methyltransferase activity
Clone rasi-1 matrix metalloproteinase RASI-1	1.70	4.56	.00019	NM_002429	Hydrolase activity
VASP, exons 4–13	1.68	4.35	.00026	NM_003370	Actin binding
Xeroderma pigmentosum, complementation group A	1.63	3.86	.00085	NM_000380	Damaged DNA binding
Urokinase-type plasminogen activator receptor; GPI-anchored form precursor *(UPAR)*; monocyte-activation antigen Mo3; CD87 antigen	1.53	4.41	.00023	NM_002659	Protein binding
Down-regulated					
Chemokine (C-C motif) receptor 2	0.35	−6.69	.00000	NM_000647	C-C chemokine receptor activity
Interleukin 7 receptor	0.47	−3.69	.00129	NM_002185	Antigen binding
Annexin II (lipocortin II)	0.49	−4.86	.00007	NM_004039	Calcium ion binding
Colony stimulating factor 2 receptor β, low-affinity (granulocyte-macrophage)	0.52	−3.85	.00088	NM_000395	Interleukin 3 receptor activity
Cytoplasmic dynein light chain	0.53	−4.12	.00046	NM_003746	Enzyme inhibitor activity
Ribosomal protein L13a	0.55	−3.94	.00070	X56932	Structural constituent of ribosome
Ikaros/LyF-1 homolog	0.56	−4.30	.00029	NM_006060	DNA binding
Chaperonin-containing TCP1, subunit 4 (Δ)	0.56	−4.60	.00014	NM_006430	Unfolded protein binding
Eosinophil Charcot-Leyden crystal (CLC) protein (lysophospholipase)	0.57	−3.73	.00116	NM_001828	Hydrolase activity
Myeloid cell nuclear differentiation antigen	0.57	−3.66	.00138	M81750	DNA binding
Ribosomal protein S16	0.59	−3.84	.00091	M60854	Structural constituent of ribosome
FK506-binding protein 4 (59 kDa)	0.62	−4.28	.00030	NM_002014	Isomerase activity
Transforming growth factor β receptor IIB	0.62	−3.87	.00082	NM_003242	Type II transforming growth factor β receptor activity
Ribosomal protein L3	0.62	−3.80	.00099	X73460	Structural constituent of ribosome
KIAA0053	0.63	−5.73	.00001	D29642.1	GTPase activator activity
Peptidylprolyl isomerase D (cyclophilin D)	0.65	−4.71	.00011	NM_005038	FK506 binding
Citrate synthase	0.66	−5.54	.00001	NM_004077	Transferase activity
FADD	0.66	−3.72	.00119	NM_003824	Protein binding
C-myc oncogene	0.66	−3.84	.00089	NM_002467	Transcription factor activity
Interferon regulatory factor 2	0.66	−3.60	.00159	NM_002199	RNA polymerase II transcription factor activity
Intercellular adhesion molecule 3	0.66	−4.30	.00029	NM_002162	Protein binding

Table 3. Gene ontology (GO) comparison to discriminate between patients with chronic hepatitis C and healthy volunteers.

GO category	GO description	Genes, no.	*P*	
			LS permutation	KS permutation
7259	JAK-STAT cascade	6	.00167	.17913
6959	Humoral immune response	25	.00303	.03114
7186	G protein–coupled receptor protein signaling pathway	18	.00348	.17617

NOTE. JAK-STAT, Janus kinase signal transducer and activation of transcription; KS, Kolmogorov-Smirnov; LS, least squares.

genes, 200 receptor- and cell adhesion–related genes, 160 apoptosis- and cell cycle–related genes, 150 transcription factors, 120 stress-response genes, and 275 other functional genes.

RNA isolation and antisense RNA amplification. Total RNA from PBMCs was isolated using Micro RNA Isolation Kits (Stratagene), and antisense RNA (aRNA) was amplified as described elsewhere [20, 22, 24]. The quality and degradation of isolated RNA were estimated after electrophoresis using an Agilent 2001 bioanalyzer. The references used for each microarray analysis were aRNA samples prepared from PBMCs obtained from a healthy volunteer. Microarray hybridization was performed as described elsewhere [19–24], and each hybridization was repeated for all samples.

Gene-expression profiles of liver-infiltrating lymphocytes in

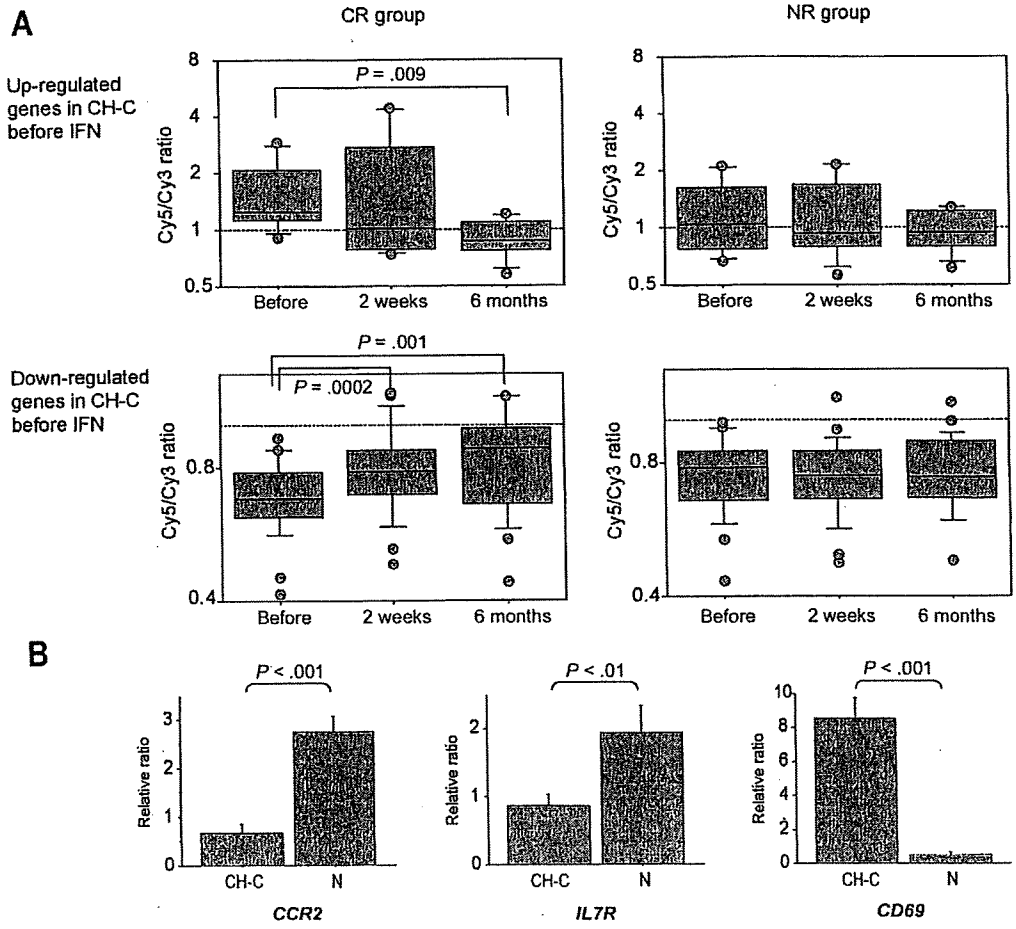

Figure 2. *A*, Changes in gene-expression profiles over the course of interferon (IFN) therapy (as shown in table 2) distinguishing patients with chronic hepatitis C (CH-C) from healthy volunteers before the start of IFN therapy. Box charts show average rates of change in relation to healthy volunteers as index functions. *B*, Real-time polymerase chain reaction data for *CCR2* and *IL7R*, which were down-regulated (as determined on the basis of microarray data) in patients with CH-C before the start of IFN therapy, and *CD69*, which was up-regulated in patients with CH-C.

patients with CH-C were investigated by laser-capture microdissection (LCM). Infiltrated lymphoid cells in the portal area and hepatocytes in liver-biopsy specimens obtained from 8 patients with CH-C were isolated by LCM. After 2 rounds of total RNA amplification, the gene expression in infiltrated lymphoid cells was compared with that in hepatocytes [25]. Optimal conditions for LCM and reproducibility of data were assessed repeatedly [24, 25]. Some of these data were used for the analysis of genes expression.

Image analysis and data processing. Quantitative assessment of signals on the slides was performed using a ScanArray 5000 device (General Scanning), followed by image analysis using QuantArray software (version 2.0; General Scanning).

Hierarchical clustering of gene expression in patients was performed using BRB-ArrayTools software (version 3.3.0; available at: http://linus.nci.nih.gov/BRB-ArrayTools.html). Filtered data were log transformed, normalized, centered, and applied to the average linkage clustering with centered correlation. BRB-ArrayTools include class comparison and class prediction tools based on univariate F tests to identify genes differentially expressed between predefined clinical groups. The permutation distribution of the F statistic, based on 2000 random permutations, was also used to confirm statistical significance. $P<$ .05, as well as >1.5-fold differences in gene expression, were considered to be significant. A gene ontology (GO) comparison tool provides a list that has more genes differentially expressed and is coordinately regulated among predefined clinical groups than expected by chance and enables findings among biologically related genes to reinforce one another. Fisher and Kolmogorov-Smirnov tests were performed for GO comparison (P <.005) (BRB-ArrayTools).

Changes in gene expression in patients receiving IFN therapy were classified on the basis of self-organizing maps (GeneCluster software; version 2.0; available at: http://www.broad.mit.edu/cancer/software/genecluster2/gc2.html).

To identify class predictor genes for IFN therapy, projective adaptive resonance theory (PART) was used as a screening method for cDNA microarray data; unlike conventional clustering methods, PART enables the elimination of nonspecific dimensions for clustering from high-dimensional data [28–30]. From the genes extracted by PART, class predictor genes were selected using a fuzzy neural network (FNN) combined with the SWEEP operator method (FNN-SWEEP method). An FNN model with 1 input unit was initially created. Expression data for genes from data sets for patients with CH-C were entered into the FNN model, and the weight parameter was determined by the SWEEP operator method. We repeated this procedure for all genes to construct a model for each gene. The 10 genes with the highest accuracy levels were selected as the "first gene." The parameter increasing method was then applied. Having the first gene fixed, we used a similar method to select the second gene, which gave the highest accuracy in combination with the first gene. Having the first gene and the second gene fixed, we selected the third gene. For validation of this model, we performed leave-one-out cross-validation (LOOCV); we left out 1 test sample and used the remaining 12 samples as training samples. We created 13 such sets. The FNN model was built up for 12 test samples, and the accuracy of training and test samples was calculated.

Real-time quantitative reverse-transcription polymerase chain reaction (RT-PCR). Quantitation of chemokine (C-C motif) receptor 2 *(CCR2), CD69,* and interleukin 7 receptor *(IL7R)* RNA expression was performed using the TaqMan real-time PCR assay (ABI PRISM 7700 Sequence Detection System; PE Applied Biosystems), as described elsewhere [22, 23].

Statistical analysis. All data are expressed as mean ± SE values. One-way analysis of variance by the Bonferroni method or Student's t test was used to determine the significance of differences in clinical characteristics between patients in this study. $P<.05$ was considered to be significant.

RESULTS

cDNA microarray analysis of expression profiles of PBMCs from patients with CH-C. We initially compared the PBMC

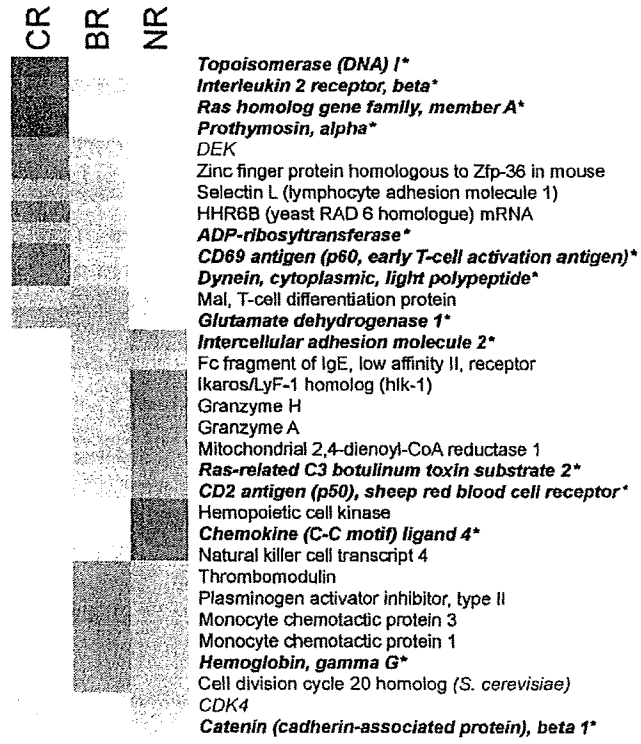

Figure 3. Thirty-two genes screened for gene-expression data before interferon (IFN) therapy by projective adaptive resonance theory. Red indicates up-regulated genes, and blue indicates down-regulated genes. Asterisks indicate genes that are included in table 4. BR, biochemical responder; CR, complete responder; NR, nonresponder.

Table 4. Ten gene combinations selected by the SWEEP operator method for construction of chronic hepatitis C class prediction at the start of interferon (IFN) therapy.

Combination	Input	Gene name	GenBank accession no.	Accuracy, %	
				Training	Test
1	1	***CD2 antigen (p50), sheep red blood cell receptor***[a]	NM_001767	21.2	14.1
	2	Glutamate dehydrogenase 1	NM_005271	72.4	46.2
	3	Dynein, cytoplasmic, light polypeptide	NM_003746	55.8	49.4
2	1	Ras-related C3 botulinum toxin substrate 2	NM_002872	34.6	20.5
	2	Glutamate dehydrogenase 1	NM_005271	81.4	68.6
	3	***Interleukin 2 receptor β***[a]	NM_000878	53.2	43.6
3	1	***Hemoglobin γG***[a]	NM_000184	19.9	16.7
	2	Ras-related C3 botulinum toxin substrate 2	NM_002872	64.7	36.6
	3	Dynein, cytoplasmic, light polypeptide	NM_003746	62.2	58.3
4	1	Intercellular adhesion molecule 2	NM_000873	28.9	26.3
	2	Ras homolog gene family member A	NM_001664	41.7	25.7
	3	Prothymosin α	NM_002823	66.0	47.4
5	1	Topoisomerase (DNA) I	NM_003286	53.9	46.2
	2	Catenin (cadherin-associated protein) β1 (88 kDa)	NM_001904	66.0	57.1
	3	Ras-related C3 botulinum toxin substrate 2	NM_002872	91.0	89.1
6	1	Catenin (cadherin-associated protein) β1 (88 kDa)	NM_001904	44.9	41.0
	2	Topoisomerase (DNA) I	NM_003286	66.0	57.1
	3	Ras-related C3 botulinum toxin substrate 2	NM_002872	91.0	89.1
7	1	Catenin (cadherin-associated protein) β1 (88 kDa)	NM_001904	35.3	31.4
	2	***Interleukin 2 receptor β***[a]	NM_000878	47.4	43.6
	3	ADP-ribosyltransferase (NAD+; poly [ADP-ribose] polymerase)	NM_001618	62.2	60.9
8	1	Chemokine (C-C motif) ligand 4	NM_002984	44.9	41.0
	2	***Interleukin 2 receptor β***[a]	NM_000878	37.8	29.5
	3	Topoisomerase (DNA) I	NM_003286	44.9	34.6
9	1	***Interleukin 2 receptor β***[a]	NM_000878	30.8	30.8
	2	Catenin (cadherin-associated protein) β1 (88 kDa)	NM_001904	47.4	43.6
	3	ADP-ribosyltransferase (NAD+; poly [ADP-ribose] polymerase)	NM_001618	62.2	60.9
10	1	CD69 antigen (p60, early T cell–activation antigen)	NM_001781	42.3	32.1
	2	Prothymosin α	NM_002823	33.3	24.4
	3	Glutamate dehydrogenase 1	NM_005271	39.1	31.4

[a] Genes that present similar expression patterns during IFN and ribavirin combination therapy.

gene-expression profiles of patients with CH-C with those of healthy volunteers. For all 1305 genes, the results of hierarchical clustering analysis, a nonsupervised learning method, confirmed that the gene-expression profiles of PBMCs from the 6 healthy volunteers clearly differed when compared with those of the 13 patients with CH-C (group A) before IFN therapy (figure 1*A*). When the 2 groups were compared by support vector machine, a supervised learning method (BRB-ArrayTools), a total of 48 predictor genes were identified with a significance level of $P < .002$, and it was possible to differentiate the 2 groups with 100% accuracy. Gene parameters (ratio, *T* value, *P* value, description, GenBank accession no., and annotation) are summarized in table 2.

A GO comparison tool (BRB-ArrayTools) identifies more genes that are differentially expressed and are coordinately regulated among predefined clinical groups than expected by chance, thus enabling the finding of biologically related genes to reinforce one another. GO comparison of gene expression between the patients with CH-C and the healthy volunteers revealed significant differences in the Janus kinase signal transducer and activation of transcription (JAK-STAT) cascade, humoral immune response, and G protein–coupled receptor protein signaling pathway ($P < .005$) (table 3). One-way clustering analyses of representative differentially expressed genes are shown in figure 1*B*. These genes were generally activated in PBMCs from patients with CH-C; however, genes such as *CCR2*, monocyte chemoattractant protein 1 receptor, and *IL7R* were significantly down-regulated. The reason for this is not known, but it may reflect infiltration of PBMCs into the liver. The top 20 differentially expressed genes were selected, and gene-expression profiling of these genes in liver-infiltrating lymphocytes was performed (figure 1*C*). Most of the gene-

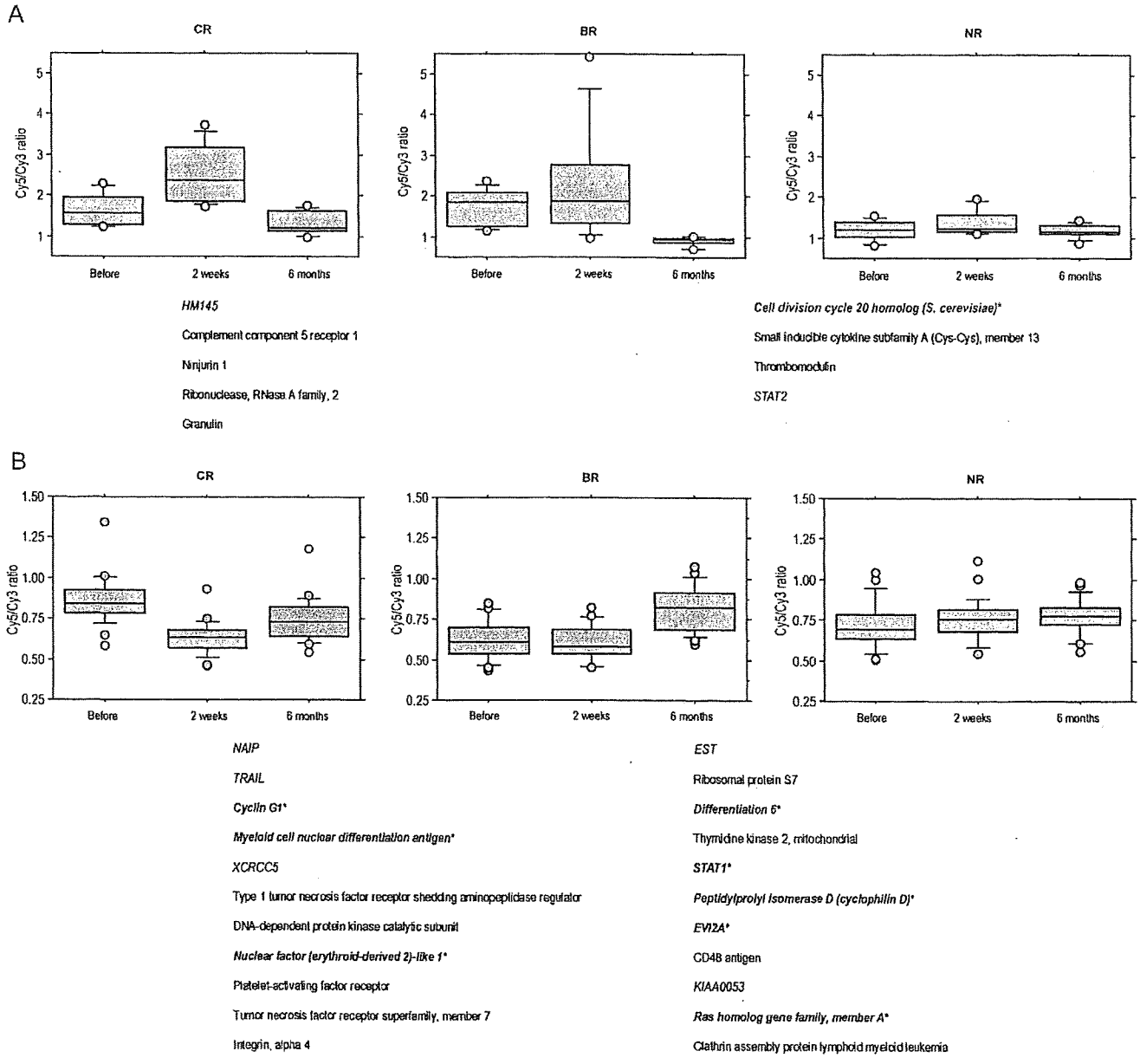

Figure 4. Gene-expression patterns. By use of projective adaptive resonance theory, 86 genes with changes in gene expression before and 2 weeks after the start of interferon (IFN) therapy were selected. For the complete responder (CR) group, changes in the expression of the 86 genes due to IFN therapy were classified into the following 5 patterns, on the basis of self-organizing maps (GeneCluster): up-regulated at 2 weeks after the start of IFN therapy and then down-regulated after the end of IFN therapy *(A)*; down-regulated at 2 weeks after the start of IFN therapy and then up-regulated after the end of IFN therapy *(B)*; up-regulated at 2 weeks after the start of IFN therapy and also up-regulated after the end of IFN therapy *(C)*; up-regulated at 2 weeks after the start of IFN therapy and then returned to normal after the end of IFN therapy *(D)*; and down-regulated at 2 weeks after the start of IFN therapy and also down-regulated after the end of IFN therapy *(E)*. Representative genes are listed under each pattern. Asterisks indicate genes that are included in table 5.

expression ratios for liver-infiltrating lymphocytes showed >1-fold increases compared with hepatocytes, thus indicating that most genes were preferentially expressed in lymphocytes. Interestingly, the genes with increased expression in liver-infiltrating lymphocytes tended to be expressed at lower levels in PBMCs (figure 1*C*).

Serial changes in the differentially expressed genes listed in table 2 during IFN treatment are shown in figure 2*A*. In the